RESERVOIR CHARACTERIZATION, FORMATION EVALUATION, AND 3D

GEOLOGIC MODELING OF THE UPPER JURASSIC SMACKOVER MICROBIAL

CARBONATE RESERVOIR AND ASSOCIATED RESERVOIR FACIES AT LITTLE

CEDAR CREEK FIELD, NORTHEASTERN GULF OF MEXICO

A Thesis

by

SHARBEL SALAM AL HADDAD

Submitted to the Office of Graduate Studies of
Texas A&M University
in partial fulfillment of the requirements for the degree of

MASTER OF SCIENCE

August 2012

Major Subject: Geology

Reservoir Characterization, Formation Evaluation, and 3D Geologic Modeling of the

Upper Jurassic Smackover Microbial Carbonate Reservoir and Associated Reservoir

Facies at Little Cedar Creek Field, Northeastern Gulf of Mexico

RESERVOIR CHARACTERIZATION, FORMATION EVALUATION, AND 3D

GEOLOGIC MODELING OF THE UPPER JURASSIC SMACKOVER MICROBIAL

CARBONATE RESERVOIR AND ASSOCIATED RESERVOIR FACIES AT LITTLE

CEDAR CREEK FIELD, NORTHEASTERN GULF OF MEXICO

A Thesis

by

SHARBEL SALAM AL HADDAD

Submitted to the Office of Graduate Studies of
Texas A&M University
in partial fulfillment of the requirements for the degree of

MASTER OF SCIENCE

Approved by:

Chair of Committee,   Ernest A. Mancini
Committee Members,   Michael C. Pope
                                  Michael J. King
Head of Department,   John R. Giardino

August 2012

Major Subject: Geology

ABSTRACT

Reservoir Characterization, Formation Evaluation, and 3D Geologic Modeling of the

Upper Jurassic Smackover Microbial Carbonate Reservoir and Associated Reservoir

Facies at Little Cedar Creek Field, Northeastern Gulf of Mexico. (August 2012)

Sharbel Salam Al Haddad, B.S., American University of Beirut; M.S., American

University of Beirut

Chair of Advisory Committee: Dr. Ernest A. Mancini

Little Cedar Creek field is a mature oil field located in southeastern Conecuh County, Alabama, in the northeastern Gulf of Mexico. As of May 2012, 12.5 MMBLS of oil and 14.8 MMCF of natural gas have been produced from the field area. The main reservoirs are microbial carbonate facies and associated nearshore high energy shoal facies of the Upper Jurassic Smackover Formation that overlie conglomerate and sandstone facies of the Norphlet Formation and underlie the argillaceous, anhydritic-carbonaceous facies of the Haynesville Formation. These carbonate reservoirs are composed of vuggy boundstone and moldic grainstone, and the petroleum trap is stratigraphic being controlled primarily by changes in depositional facies. To maximize recovery and investment in the field, an integrated geoscientific-engineering reservoir-wide development plan is needed, including reservoir characterization, modeling, and simulation. This research presents a workflow for geological characterization, formation evaluation, and 3D geologic modeling for fields producing from microbial carbonates

and associated reservoirs. The workflow is used to develop a 3D geologic model for the carbonate reservoirs. Step I involves core description and thin section analysis to divide and characterize the different Smackover facies in the field area into 7 units. The main reservoir facies are the microbial boundstone characterized by vuggy porosity and nearshore/shoal grainstone characterized by moldic porosity. Step II is well log correlation and formation evaluation of 113 wells. We use wireline logs and conventional core data analysis data to calculate average porosity values, permeability and water saturations. Neural networks are utilized at this stage to derive permeability where core measurements are absent or partially present across the reservoirs. Step III is building the 3D structural and stratigraphic framework that is populated with the petrophysical parameters calculated in the previous step. Overall, the integration of reservoir characterization, formation evaluation, and 3D geologic modeling provides a sound framework in the establishment of a field/reservoir-wide development plan for optimal primary and enhanced recovery for these Upper Jurassic microbial carbonate and associated reservoirs. Such a reservoir-wide development plan has broad application to other fields producing from microbial carbonate reservoirs.

DEDICATION

To my family, friends, and my beloved girlfriend

ACKNOWLEDGEMENTS

TABLE OF CONTENTS

LIST OF FIGURES

LIST OF TABLES

INTRODUCTION

The Upper Jurassic (Oxfordian) Smackover Formation is the most prolific

hydrocarbon producing formation onshore Alabama. Oil and gas are produced from

structural, stratigraphic and combination settings. Since the discovery of Toxey Field in

1967, over 100 Smackover fields have been developed in southwest Alabama (Alabama

State Oil and Gas Board, 2010). The Smackover's hydrocarbon reservoir potential in the

northeastern Gulf of Mexico was discussed and described extensively by Mancini and

Benson (1980), Baria et al. (1982), Crevello and Harris (1984), Markland (1992),

Benson et al. (1996), Kopaska-Merkel (1998, 2002), Hart and Balch (2000), Parcell

(2000), Mancini and Parcell (2001), Llinas (2004) and Mancini (2004). Mancini et al.

(2004) compared and classified microbial buildups of the Smackover to Jurassic buildup

outcrops in Spain and Portugal. They interpreted them to have developed in normal-

marine conditions on middle and outer ramp settings (10-400 m of water depth). These

buildups commonly developed on Paleozoic crystalline (elevated igneous and/or

metamorphic) paleotopographic features (Mancini et al., 2004). The microbial features

in the Smackover fields are usually directly overlain by high energy, nearshore facies

forming a single Smackover reservoir. Prior to discovery of the Little Cedar Creek field

(Figure 1), exploration strategies focused on locating the Smackover reservoirs on

paleotopographic highs associated with Paleozoic crystalline basement rocks (Figure 2;

_____

This thesis follows the style of American Association of Petroleum Geologists.

Mancini et al., 2008). Utilizing 3-D reflection data was a key to major

discoveries in the Smackover (Llinas, 2004; Mancini et al., 2000, 2004). The seismic

data would be used to identify paleotopographic anomalies for exploration targets. The

data would be further used to predict whether reservoir facies developed on both the

crest and flanks of a paleohigh or only on the flanks of the feature for further

development of the discovered fields (Mancini et al., 2003, 2004, 2006, 2008).
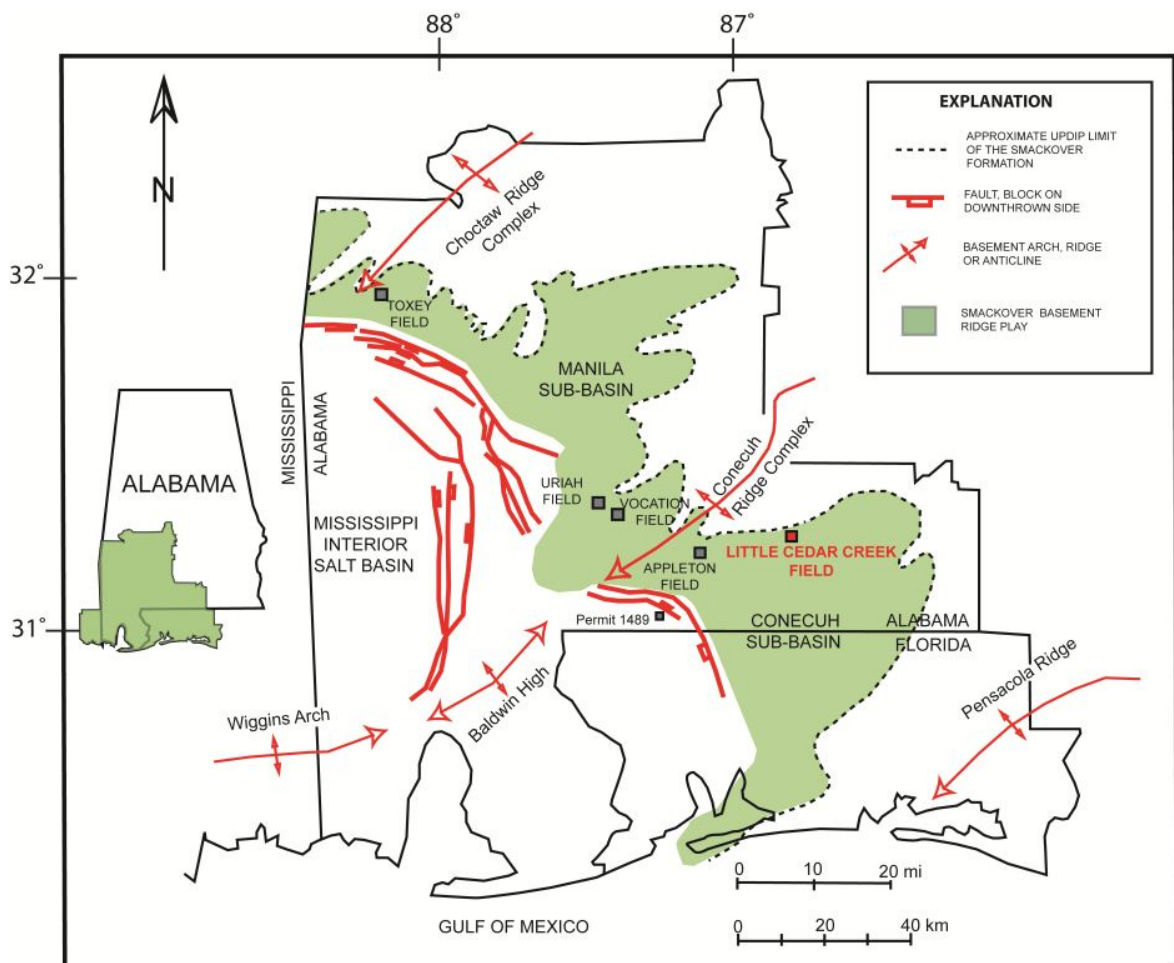
Figure 1. Location map of the Little Cedar Creek field. Note the location of major structural features and key Smackover fields, including the Little Cedar Creek field (after Mancini et al., 2008).
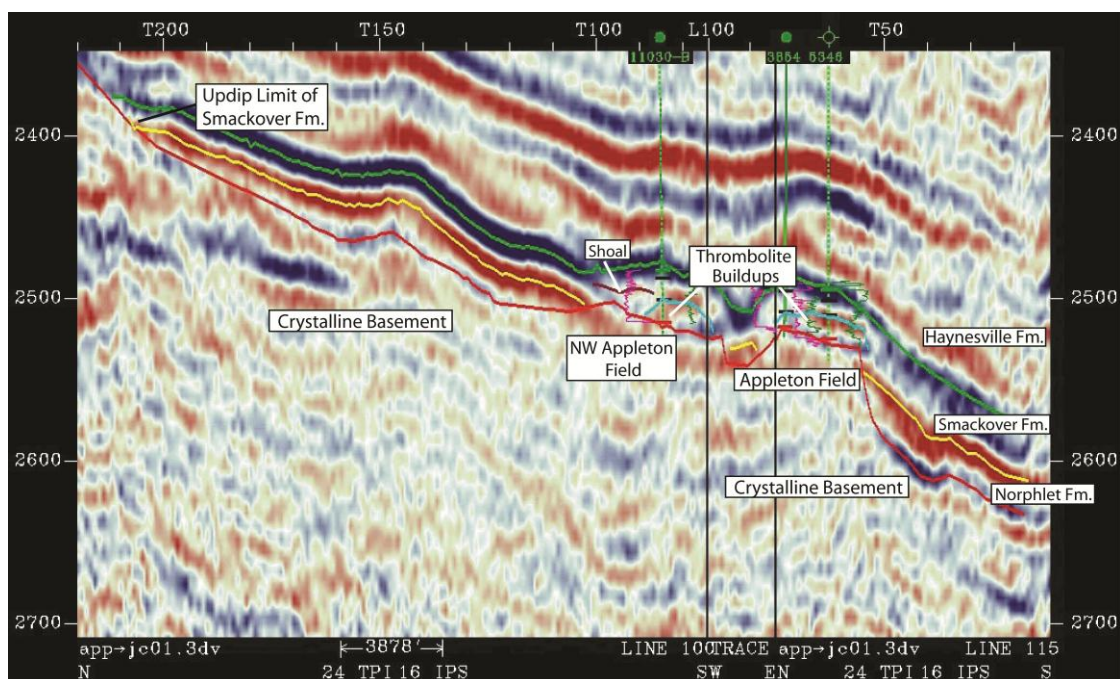
Figure 2. Seismic profile oriented in an approximate dip direction showing the updip limit of the Smackover in northeastern Gulf of Mexico. Note that the Little Cedar Creek field occurs near the updip deposition limit of the Smackover on this line (adapted from Mancini et al., 2004).

However and unlike most Smackover producing fields in southwestern Alabama, Little Cedar Creek field is producing from two independent reservoirs. The upper reservoir, nearshore high-energy oolitic grainstone and packstone, and the lower reservoir, microbial boundstone, are separated vertically by a deeper water subtidal lime mudstone (Mancini et al., 2008). Moreover, the field lacks the structural component of the combination traps associated with basement paleohighs, and the reservoirs are characterized by the preservation of primary depositional fabric (Mancini et al., 2008). Within the field, the Upper Jurassic Smackover Formation unconformably overlies conglomerate and sandstone facies of the Norphlet Formation and is overlain by the argillaceous, anhydritic carbonaceous facies of the Haynesville Formation. Mancini et al.

(2008) and Ridgway (2010) identified the microbialites (thrombolites) of the Little Cedar Creek field to have developed updip, within 5 km (3 miles) of the Smackover paleoshoreline (Figure 2; Mancini et al., 2008). The growth of these buildups is directly influenced by water depth, subtle topographic highs of the Norphlet Formation, low sedimentation rate, and tranquil marine conditions (Mancini et al., 2008; Ridgway, 2010). They also concluded that the exploration and development strategies for Smackover reservoirs need to be refined. The new refined strategies would need to incorporate and integrate data from detailed regional geology, logging, coring, and testing of the drilled wildcat wells (Mancini et al., 2008). Moreover heterogeneity and connectivity within the reservoirs should be assessed using detailed geologic, petrophysical, geochemical, and engineering studies of wire-line log, core, and well-test data (Mancini et al., 2008). This would be attained through reservoir characterization, performance analysis, and modeling studies (Mancini et al., 2008).

This paper builds on the work of Mancini et al. (2008) and Ridgway (2010). The main objective is a scientific integration of reservoir characterization, formation evaluation, and 3D geologic modeling that provides a sound framework in the establishment of the field/reservoir-wide development plan. The results of this work contribute to further the understanding of the reservoir heterogeneities, the spatial distribution of flow units, and the identification of baffles and barriers to flow in the Little Cedar Creek field and to enhance exploration and development strategies in the field and similar microbial carbonate reservoir fields in the Gulf of Mexico.

Location and Field History

The Little Cedar Creek field is located approximately 10 miles southeast of Evergreen, in Conecuh County, Alabama (Figures 1 and 3). In 1994, Hunt Oil Company drilled the first discovery well in Section 30, Township 4 North, Range 12 East, in Conecuh County, Alabama. The well was the 30-1 #1 Cedar Creek Land and Timber Company well (Permit #10560) and was drilled to a total depth of 12,100 feet in the Smackover Formation. The well tested at 108 BOPD of 47 degree API gravity oil. In 2000, Midroc Operating Company purchased all area leases from Hunt Oil before Sklar Exploration Company, LLC and Colombia Petroleum LLC became the second and third operators in 2006 and 2008, respectively. To date, Midroc and Sklar have drilled over 113 wells in the area, producing 12.5 MMBLS of oil and 14.8 MMCF of natural gas making the Little Cedar Creek field one of the best Smackover oil-producing fields in the State of Alabama. In January 1, 2005 the western portion of the Little Cedar Creek field was unitized*. In October 2007, Midroc Operating Company started a gas-injection secondary recovery project in the unitized portion of the field. The recovery project targeted the upper reservoir of the field and response to the gas injection steadily increased the annual oil production from the field since 2008, and this production is primarily responsible for reversing the declining trend in the state's oil production (Alabama State Oil and Gas overview report, 2009).

*Unitization is the combination of multiple wells to produce from a specified reservoir

Figure 3. Base map of Little Cedar Creek field, Conecuh County, Alabama.

Geologic Setting

The geologic history of the Little Cedar Creek field area is directly related to the evolution of the Mississippi interior salt basin of the northeastern Gulf of Mexico during the Mesozoic time. Active rifting (Stage 1) and drifting (Stage 2) during the opening of

Gulf of Mexico from the late Triassic to Cretaceous, controlled the depositional styles in the region (Winkler et al., 1988; MacRae et al., 1993; Mancini et al., 2001; Pindell, 2010). Mancini et al. (2003) classified the Mississippi interior salt basin as the interior fracture portion of a marginal sag basin according to the basin classification of Kingston et al. (1983). In the Late Jurassic, sea-floor spreading and new oceanic crust emplacement in the deep central Gulf of Mexico resulted in a regional marine transgression (Figure 4; Mancini et al., 2001; 2008). The transgression was accompanied by crustal cooling and subsidence, the termination of the wide-scale salt deposition, and the transition from restricted marine to open marine depositional environment (MacRae et al, 1993, Yurewicz et al., 1993; Mancini et al., 2001). Basin subsidence and erosion of the southern Appalachian Mountain chain during the Callovian and Oxfordian stages of the Upper Jurassic resulted in the widespread deposition of the Norphlet Formation (Mancini et al., 1985; Salvador, 1987; Markland, 1992; Llinas, 2004). The Norphlet is composed of conglomerate, sandstones, red bed, and shale that were deposited in alluvial fan and fluvial systems in the updip areas proximal to its provenance, whereas eolian processes governed Norphlet deposition downdip, away from the Appalachian Mountain front (Mancini et al., 1985). The Norphlet reaches a maximum thickness of approximately 450 meters (1475 feet) in the areas of central Mississippi, southern Alabama, western Florida panhandle and parts of the offshore Gulf of Mexico shelf area. The Norphlet is approximately 30 meters (98 feet) thick along the northern and northwestern rims of the basin (Mancini et al., 1985; Salvador, 1987). On a carbonate ramp surface, intertidal to subtidal laminated lime mudstones, subtidal peloidal

wackestone and packstone, subtidal to intertidal peloidal, ooid, oncoidal packstone and

grainstone interbedded with laminated and fenestral lime mudstones were deposited in

the Smackover Formation (Mancini et al., 2001). Smackover microbial reefs developed

on the ramp surface (Dobson, 1990; Dobson and Buffler, 1997; Mancini et al., 2001). In

Southwestern Alabama, the Smackover consists of three general lithofacies (Mancini

and Benson, 1980; Mancini et al., 1990; Baria et al. 1982; Bradford, 1984; Benson,

1988). A lower member representing the initial phase of marine transgression consists

of algal laminites, intraclastic wackestone/packstone, and peloidal-oncoidal

packstone/wackestones (Benson, 1988). It was deposited in intertidal to shallow sub-

tidal environments (Benson, 1988). A middle member composed of skeletal-peloidal

wackestones interbedded with organic-rich, laminated mudstones, was deposited in deep

ramp to basinal environments during later stages of the transgression and the initial

stages of aggradation in late Callovian time (Baria et al., 1982; Benson, 1988). An upper

member of cyclic coarsening upward sequences of peloidal, oncoidal, and oolitic

packstone and grainstone, that formed during the early Oxfordian highstand aggradation

and pro-gradation of shallow water shoal and tidal-flat complexes (Ahr, 1973; Baria et

al., 1982; Benson, 1988). The Smackover paleotopograhy such as Wiggins arch,

Choctaw ridge, Conecuh ridge, salt ridges, and basement paleohighs controlled

Smackover thickness and depositional patterns in Southwestern Alabama (Benson, 1988;

Mancini et al., 2008). The Smackover Formation overlies the Norphlet Formation and is

overlain by the Haynesville Formation in the northeastern Gulf of Mexico. Locally, it

disconformably overlies the Norphlet Formation. The Haynesville Formation includes

Interbedded anhydrite, limestone, shale, and sandstone (Tolson et al., 1983; Mann, 1988;

Mancini et al., 2001).

Figure 4. Sequence stratigraphy of Smackover Formation in Little Cedar Creek field- Alabama (modified from Mancini et al., 2008)

METHODOLOGY

Through March 2012, approximately 113 wells were drilled in Little Cedar Creek field (Appendix 1).Well logs, well surveys, and conventional core data analysis were used in this study and are available through the Geological Survey of Alabama- State Oil and Gas Board. 2D seismic lines throughout the field could be obtained through an independent leasing company. However 3D seismic data is not available and/or not made public therefore, the use of 2D seismic lines would not add incremental value to the current study because of resolution issues due to the subsurface depth of the reservoir (11,000 to 12,000 feet) and the thin (5-20 feet) reservoir intervals. Fortunately in the Little Cedar Creek field area, most of the wells were cored and conventional core data analysis was performed (Appendix 1). Conventional core analysis reports provide porosity, permeability, water saturation and oil saturation data for each well. The wireline log data are either in Raster Format or LAS files. Core description, thin section study, and well log analysis are the principal means to determine lithofacies. Gamma ray, neutron porosity, and density porosity curves from geophysical wireline logs were used to pick formation tops for the Smackover and Norphlet formations. The wireline logs are limestone calibrated by the service companies. Thus, density-neutron porosity curves overlay when moving through limestone unit and the curves separate where a different lithology is encountered, such as anhydrite or sandstone (Figure 5). Neutron porosity is greater than density porosity by approximately 14 units compared to anhydrite. The separation is less with sandstone, with neutron porosity greater than

density porosity by 6-8 units (Asquith and Krygowski, 2004). Gamma ray signature, porosity values, and the relative position of the density and neutron porosity curves are used to assist in characterizing lithofacies in Little Cedar Creek field (Mancini et al, 2008; Ridgway, 2010).

Ahr (2008) developed a new porosity classification scheme that considers the genetic origin of pores to characterize porosity. The triangular classification places the origin of porosity into: depositional, diagenetic, or fracture end points (Figure 5; Ahr, 2008). In general, spatial distribution of porosity is related to depositional facies boundaries when digenesis is absent. However modified diagenetic porosity changes the prediction of the distribution. Understanding carbonate reservoir characterization leads to recognition of the different processes by which porosity is formed, particularly with microbial carbonate reservoirs. Thus, the Ahr (2008) scheme was used to identify and to classify porosity and identify flow units in Little Cedar Creek field.

Data editing and preparation are important steps in the formation evaluation process. These steps are necessary to ensure that all well logs and core data are referenced to the same depth. The data editing process for this project was done in a two-step process. The first step involved choosing a base log that was assumed to have the most accurate depth to which all other logs and core data could be aligned. The resistivity log (dual induction log or dual laterolog) is usually used as the base log.
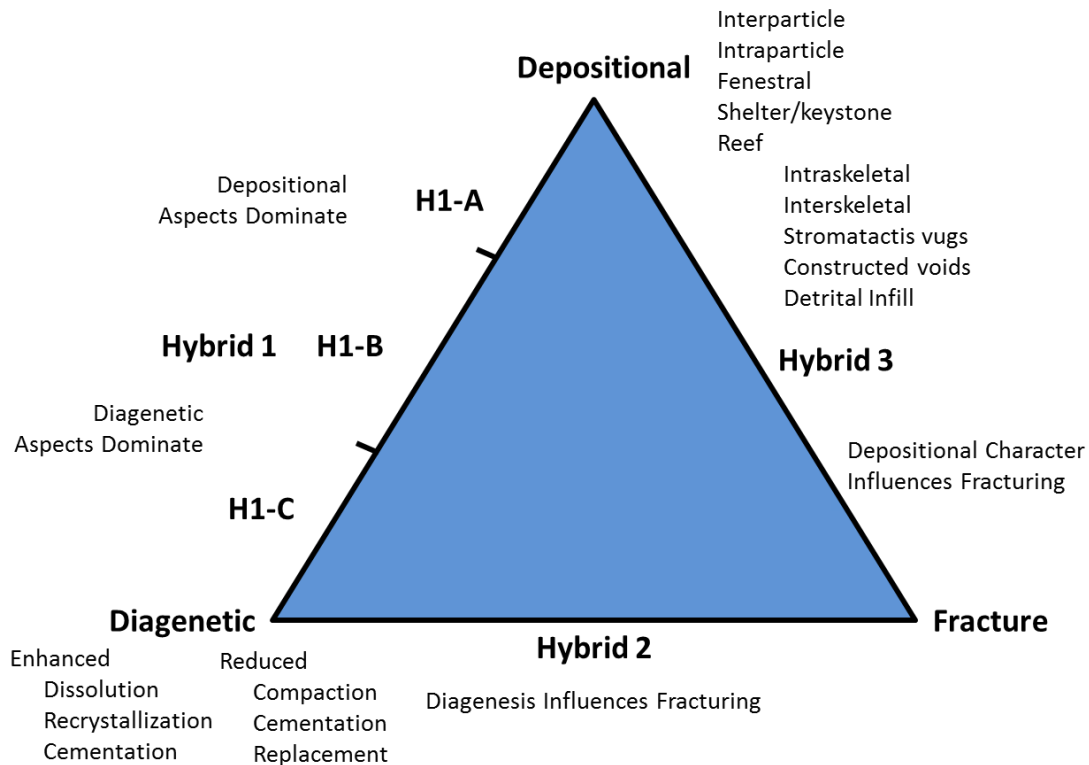
Figure 5. Ahr (2008) genetic porosity classification.

However, the gamma gay log was chosen as the base log in this project due to its ability to provide a unique signature for lithologic changes in the Smackover Formation. By comparing the Gamma Ray log to the other logs for each well, it was determined that no significant depth shifts were required. The next step in the data editing process was the integration of core data to well log data. Core porosity was compared to log-derived corrected porosity and then vertically adjusted to obtain the best match. A perfect match was not expected because of the differing value scales of the core analysis and logging tools. The core-derived porosity is obtained by measuring the porosity of a limited volume of the reservoir (volume of core) whereas wireline logging tools measure an average porosity of a relatively larger volume of reservoir (Halliburton's Open-hole Log

Analysis and Formation Evaluation, 2004). The reservoir volume effectively

investigated by the logging tools depends on the capacity of those tools, in regards to

vertical resolution and depth of investigation. The resulting depth shifts for the core data

are shown in Appendix 1. Figure 6 shows the log-derived corrected porosity on a type

log and the shifted core porosity to match the log-derived value. Average porosity, log

permeabilities and water saturation were then derived for all the wells. A complete

description of the process involved in calculating these petrophysical values is discussed

in detail in the formation evaluation section below.

The reservoir characterization data and complete formation evaluation are then

used to build the static model, and populate the grid with the lithofacies and

petrophysical facies. The final model is upscaled and exported for reservoir simulation

and history matching purposes. The stratigraphic grid was built to conform to the

geology in the field. Facies vertical tends curves and petrophysical data (porosity and

permeability) were then populated in the property modeling phase.
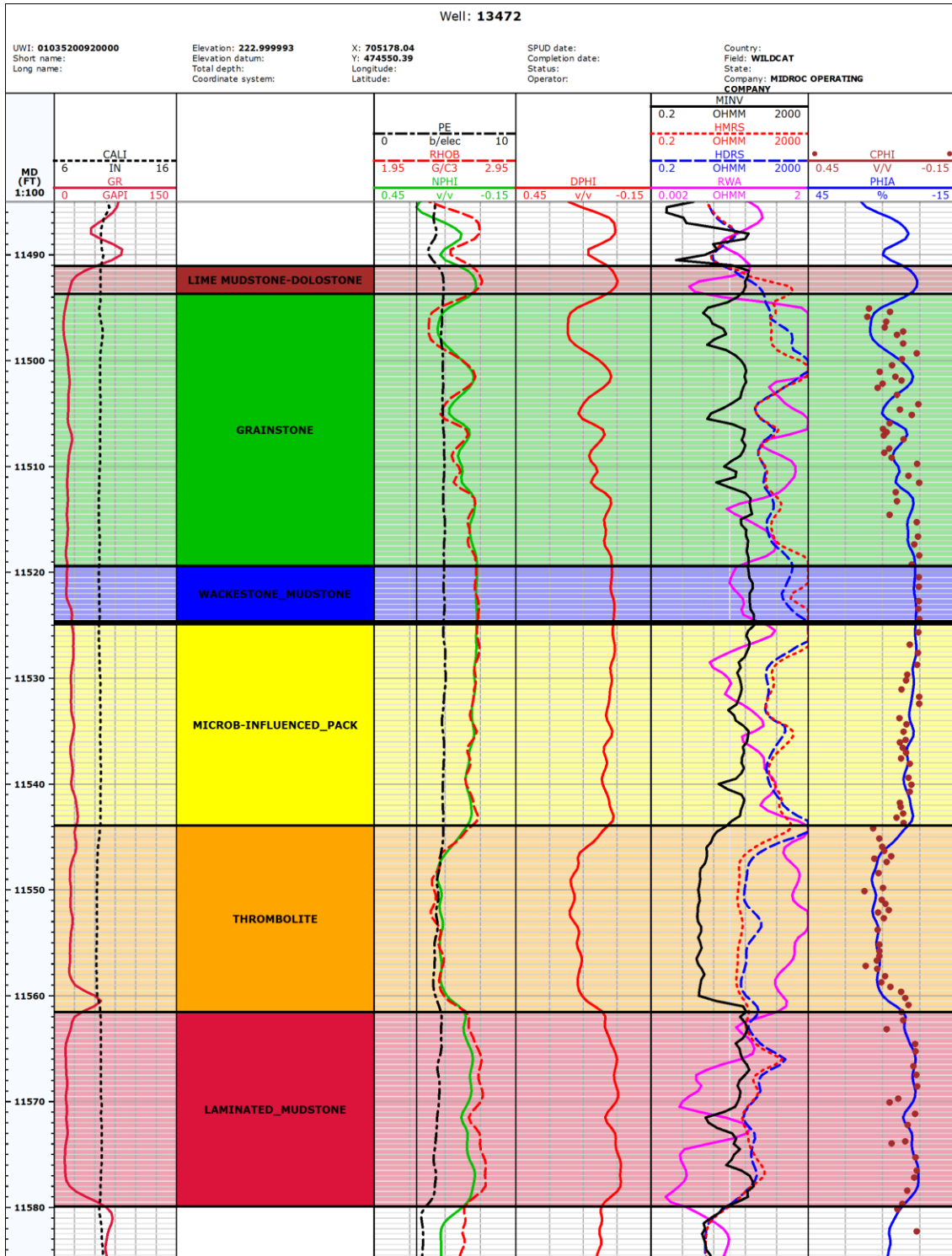
Figure 6. Type log of the Little Cedar Creek field showing a sample of the log suites available fpr this study.

RESERVOIR CHARACTERIZATION

In the Little Cedar Creek field area, the Smackover Formation ranges from 18 to 36 m (58 to 117 feet thick; Mancini et al., 2008). The Smackover Formation in the area is divided into seven distinct lithofacies (Mancini et al, 2008; Ridgway, 2010). Beginning from the top of the Smackover (Figure 4), the facies are: (S-1) peritidal lime mudstone-dolomudstone to wackestone; (S-2) tidal channel grainstone rudstone; (S-3) peloid-ooid nearshore high energy/ shoal grainstone-packstone; (S-4) subtidal wackestone-lime mudstone; (S-5) microbially-influenced packstone-wackestone; (S-6) microbial (thrombolite) boundstone; and (S-7) transgressive lime mudstone-dolomudstone. The microbial carbonate facies (thrombolite facies) and associated high energy nearshore facies (ooid peloid grainstone-packstone) are the two main producing reservoirs.

Detailed description of the facies is provided by Mancini (2006) and Ridgway (2010). The peritidal facies (S-1) is grey to light grey mudstone to wackestone lime dolostone with dolomite, anhydrite, and gypsum as accessory minerals. The facies is 0 - 25 feet thick and extends over the entire study area (Figures 7- 14) and is interpreted to have been deposited in an intertidal to subtidal, low-energy, lagoon environment (Mancini 2006; Ridgeway, 2010). The tidal channel facies (S-2) is grey rudstone to conglomerate grainstone with rounded to sub-rounded monocrystalline and polycrystalline quartz and volcanic pebbles. This facies is 10- 22 feet thick; it has sparry calcite cement, and only occurs in section 5, T5N, R13E, where it overlies the subtidal

S-4 lime wackestone (Ridgway, 2010). This facies is interpreted as having been

deposited in a high energy tidal channel environment (Mancini 2006; Ridgeway, 2010).

Because of its limited areal extent this facies is not included in the reservoir modeling.

The nearshore high energy shoal facies (S-3) includes partially dolomitized limestone

with accessory calcite and minor dolomite rhombs. This ooid, oncoidal, peoloidal,

bioclastic grainstone-packstones is tan to grey in color and have high, bimodal

(intergranular and intragranular-to-moldic) porosity. This facies is interpreted as being

deposited in higher-energy, subaqueous, subtidal shoal environments (Mancini 2006;

Ridgeway, 2010). The facies constitutes the upper reservoir in Little Cedar Creek field

and is 0- 35 feet thick (Figure 15). It has a southwest to northeast distribution (Figures 7,

8, 9 and 15) and is absent in the northeast part of the field. The subtidal wackestone-

lime mudstone facies (S-4) is a grey to dark grey limestone with calcite cement,

stylolites, microstylolites and fractures. The facies is 0-112 feet thick and is distributed

over the whole field (Figures 8- 14). These beds serve as the vertical and lateral seals to

the lower microbial reservoir (Figures 8, 9, 11 and 13). The facies is interpreted as being

deposited in a "relatively deeper"-water (<10 feet), subtidal marine environment. The

microbially-influenced packstone-wackestone facies (S-5) is a grey to dark grey

limestone with some accessory dolomite and a calcite cement. This facies occurs

throughout the field area. The packstone is a reservoir in parts of the field and while the

wackestone to lime mudstone form an updip lateral seal in the northeastern area of the

field. This unit is 0-34 feet (Figures 8- 13) thick and was deposited in subtidal

conditions in a marine environment (Ridgeway, 2010). The microbial (thrombolite)

boundstone facies (S-6) is grey to light-grey and tan limestone with accessory dolomite with clotted peloid clusters, with fine, subangular silt. These beds contain peloids, benthic foraminifera, micritized pellets, algal filaments, and *Parafavareina* pellets. The deposits are cemented with sparry calcite and characterized by 0-30 % vuggy porosity. The facies is 0-40 feet thick, being thickest in the localized major microbial buildup area that trends southwest to northeast (Figures 10, 12, 14 and 16). This facies is interpreted as being deposited in a low-energy subtidal (<10 feet) in an inner carbonate ramp environment (Ridgway, 2010). Structural maps drawn on top of the Norphlet and Smackover Formations (Figures 17 and 18) show that the northeast to southwest trending dip of the Norphlet Formation follows Ahr's (1973) carbonate ramp model. Moreover, no localized elevated features are evident on the Norphlet structure map meaning that the paleogeography was not a controlling factor in the deposition of the microbial (thrombolite) facies (S-6) and the structural closure in the field is absent. The transgressive lime mudstone and dolomudstone facies (S-7) facies is grey to reddish pink limestone and dolostone with localized dolomite, silt and sparry calcite cement. This unit has a laminated to mottled fabric with characteristic peloidal clots suggesting microbial influence and evidence of bioturbation (Ridgway, 2010). The unit is 5-55 feet thick and occurs across the entire study area (Figures 7-14). They were deposited during a relatively rapid marine transgression during the Oxfordian (Ridgway, 2010).

Figure 7. Base map of the Little Cedar Creek field in Alabama showing the location of wells available for this study.

Figure 8. A southwest- northeast structural cross section AA' of the Little Cedar Creek field showing the updip limit of the facies. Note the thinning and absence of the peloid-ooid nearshore high energy/ shoal grainstone-packstone (S-3) facies to the northeast.

Figure 9. Cont'd southwest- northeast structural cross section of the Little Cedar Creek field.
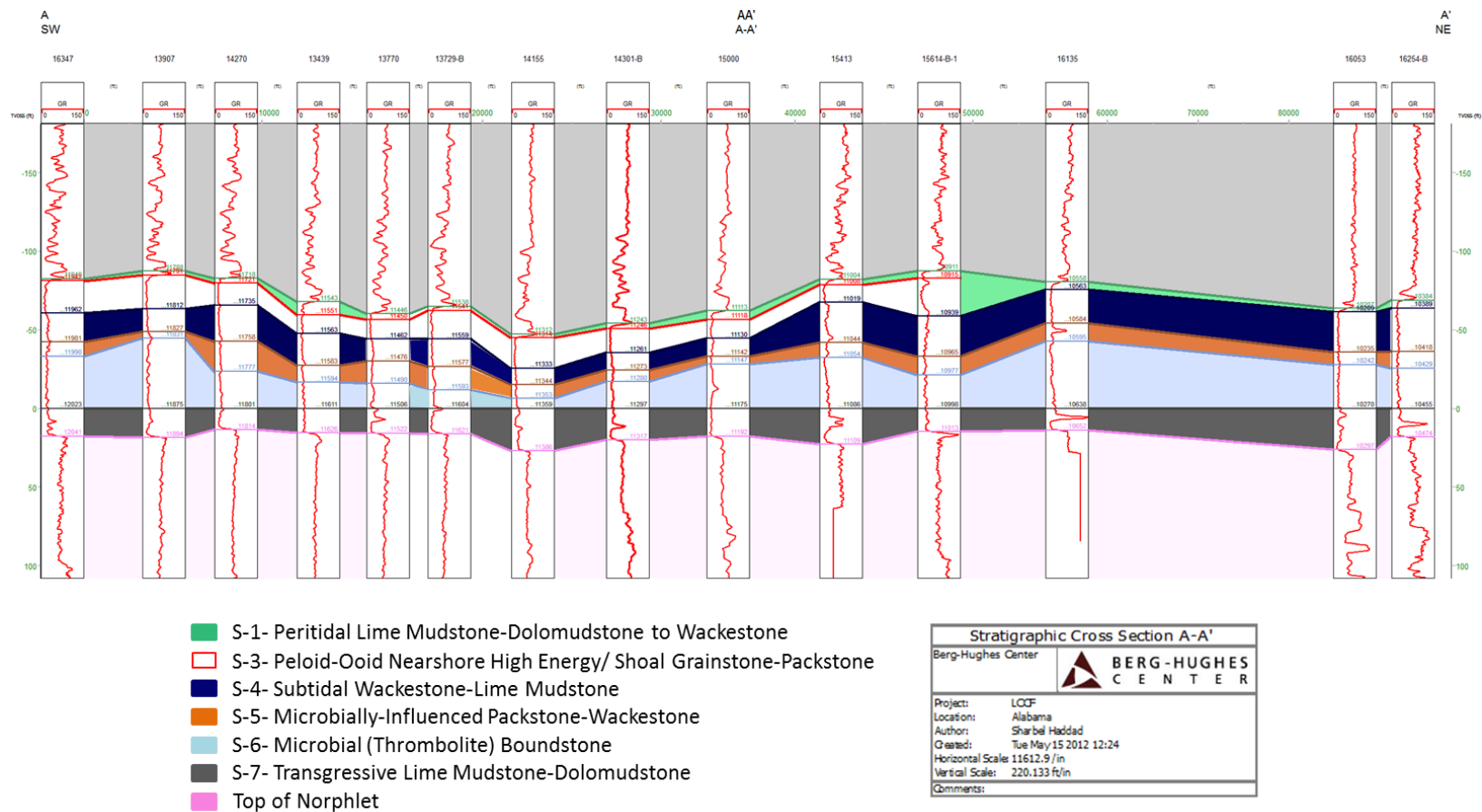
Figure 10. Stratigraphic cross section AA' showing the facies recognized in the Little Cedar Creek field area. Note the microbial (thrombolite) buildups and associated lower boundstone and packstone reservoir facies are interbedded with three lime mudstone and wackestone, and dolostone units, which serve as lateral and vertical seal beds.
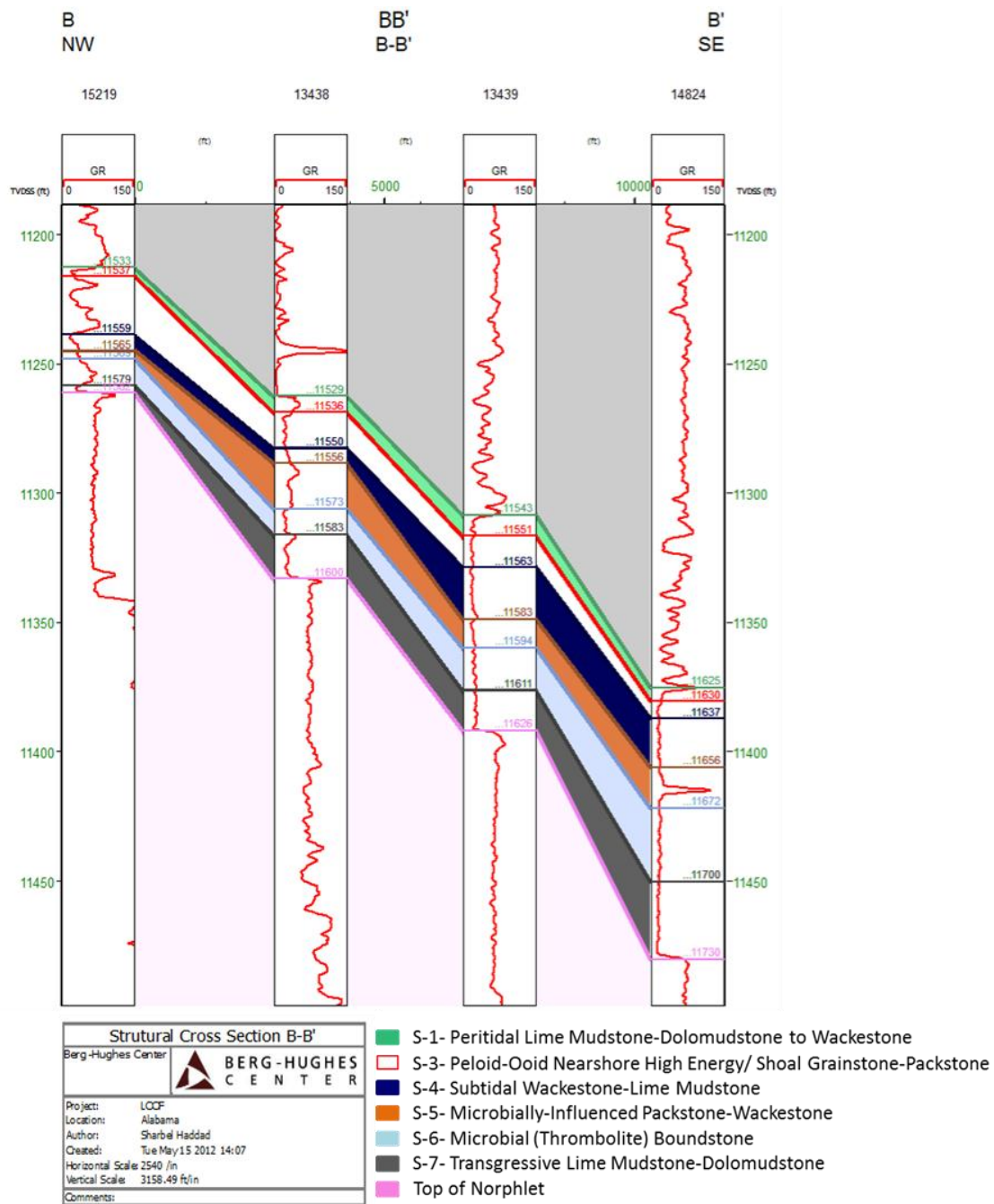
Figure 11. A northwest- southeast structural cross section BB' of Little Cedar Creek field.
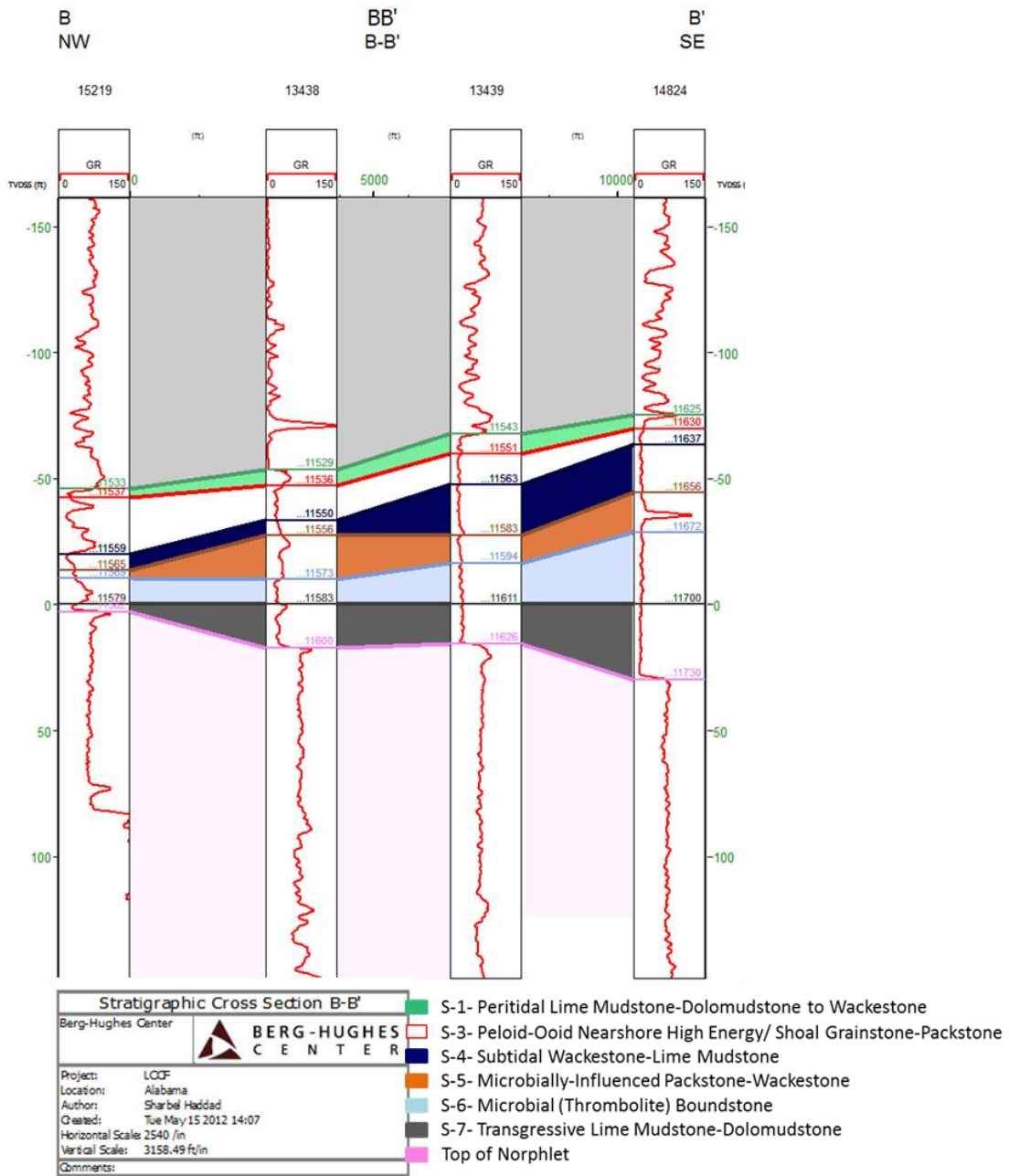
Figure 12. A northwest- southeast stratigraphic cross section BB' of Little Cedar Creek field. Note the microbial (thrombolite) buildups thickening to the center of the field.
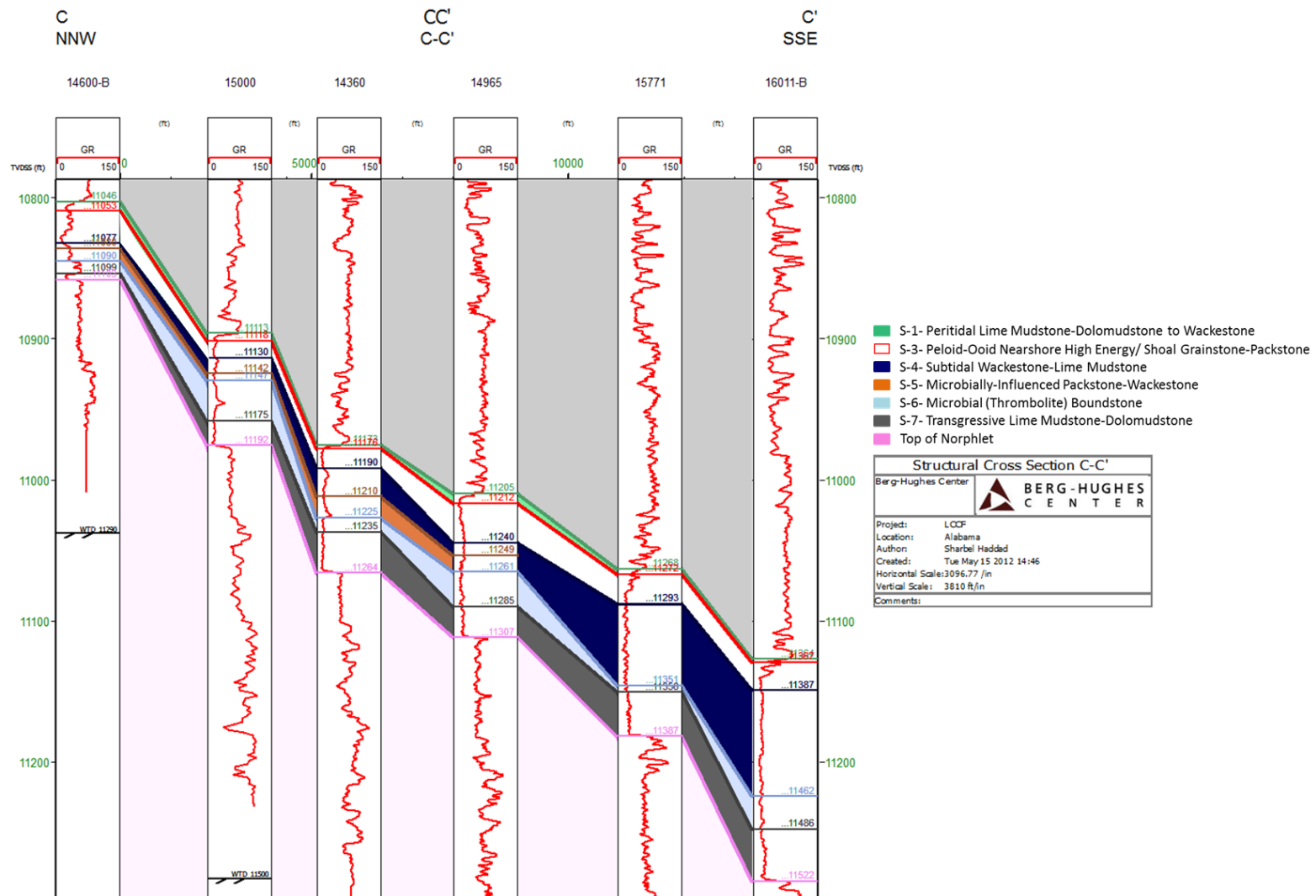
Figure 13. A north northwest- south southeast structural cross section CC' of Little Cedar Creek field.
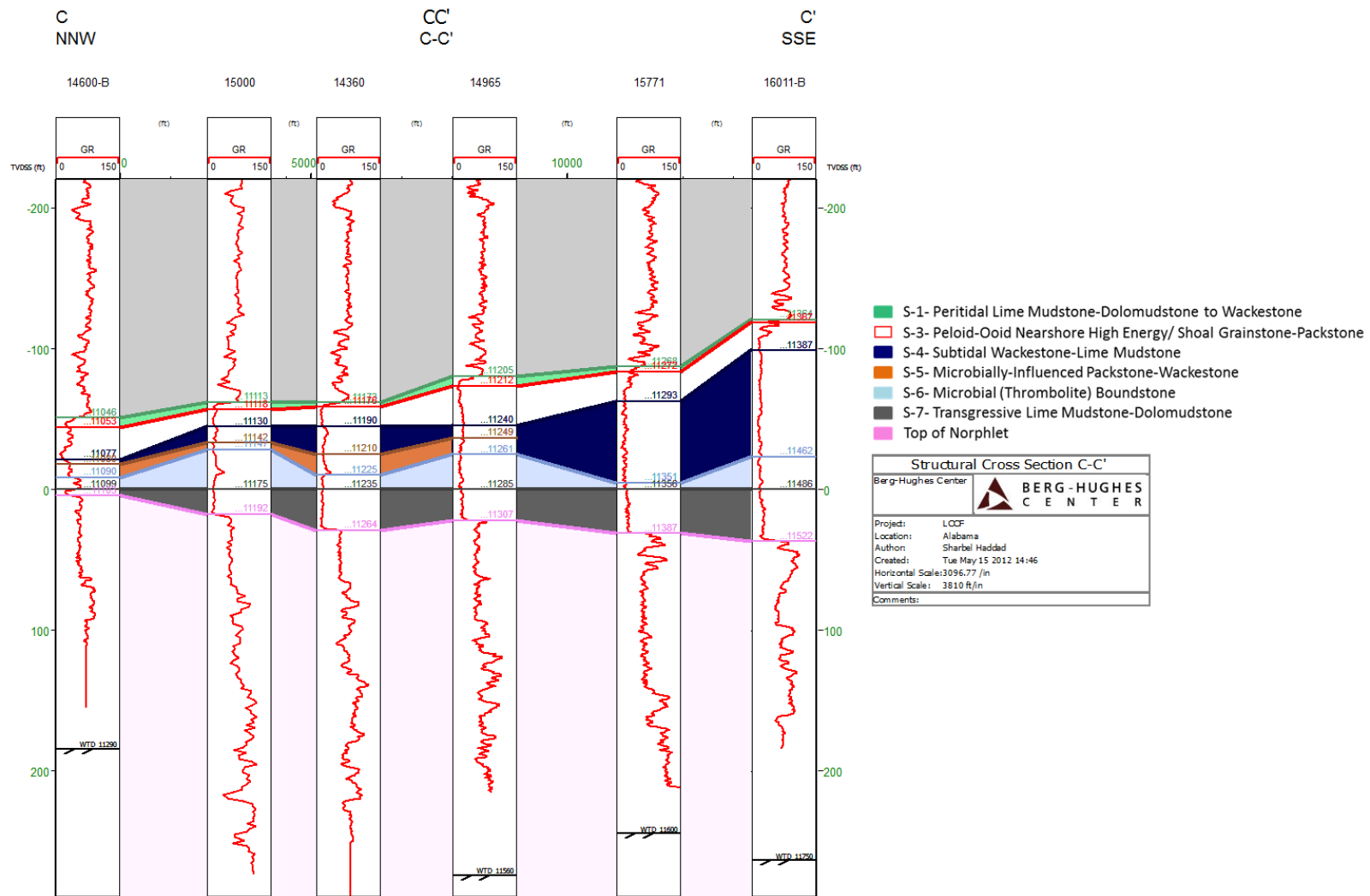
Figure 14. A north northwest- south southeast stratipgraphic cross section CC' of Little Cedar Creek field.
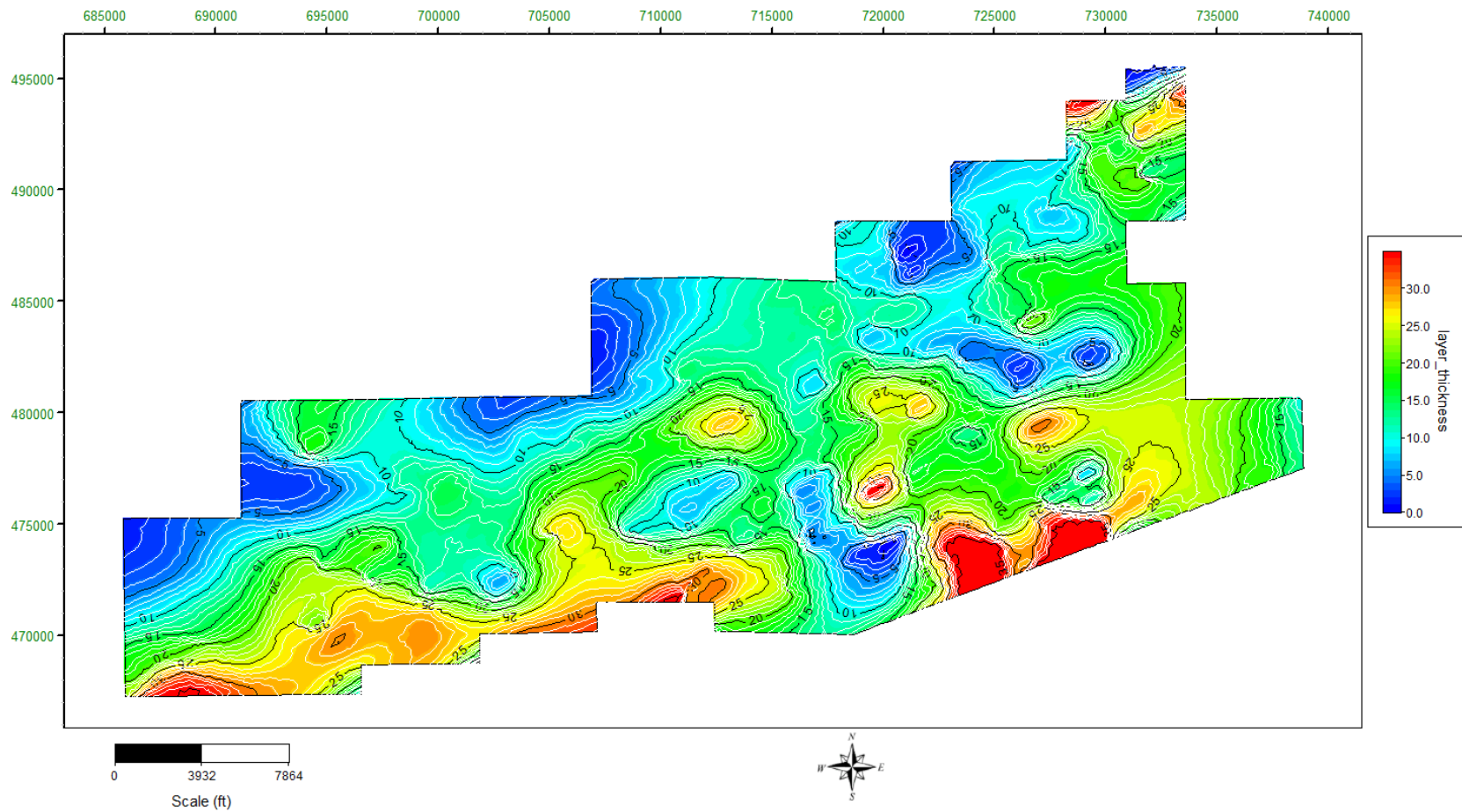
Figure 15. Isopach contour map of the peloid-ooid nearshore high energy/ shoal grainstone-packstone facies (S-3) in Little Cedar Creek field. This facies is thickest to the south and southwest and absent to the northeast.
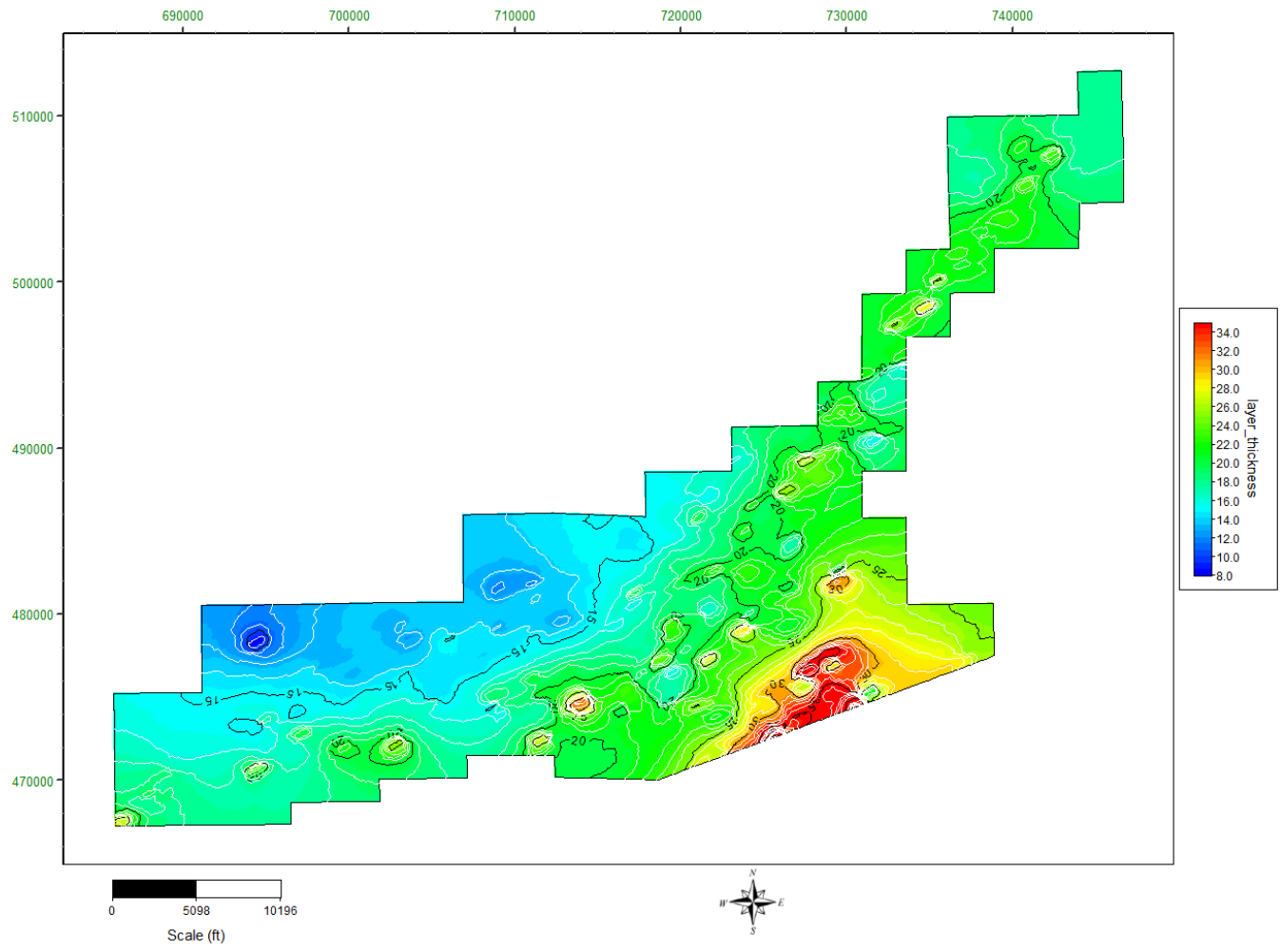
Figure 16. Isopach contour map of the microbial (thrombolite) boundstone (S-6) facies in Little Cedar Creek field. This facies is thickest to the south with localized buildups in the central and north parts of the field.

Figure 17. Structural contour map on the top of the Smackover Formation. Contour interval is 40 feet.
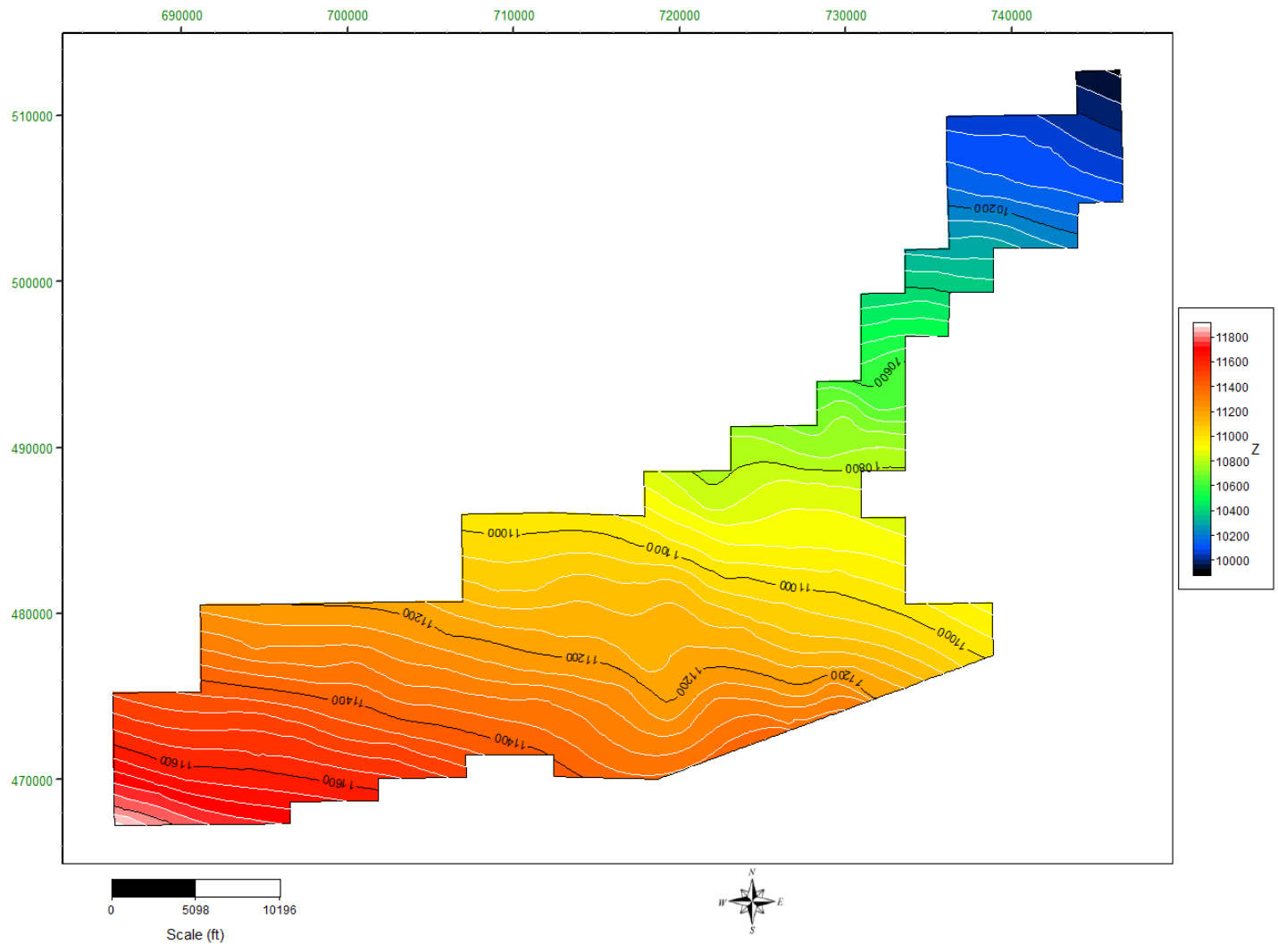
Figure 18. Structural contour map on the top of the Norphlet Formation. Contour interval is 40 feet.

The porosity in the upper grainstone-packstone reservoir facies (S-3) is solution enhanced intergranular and intragranular primary porosity and secondary moldic porosity. These reservoir beds contain ooid, peloidal, bioclastic, and oncoidal allochems that are totally to partially leached resulting in solution enhanced intergranular and intragranular to moldic porosity. According to the Ahr (2008) porosity classification, carbonates characterized by moldic pores are classified as Hybrid 1A (if depositional aspects dominate) to Hybrid 1B (if diagenetic aspects dominate; Figure 19). These reservoirs are classified as Hybrid 1A using the Ahr (2008) classification.

The lower reservoir, microbially-influenced packstone (S-5) and microbial (thrombolite) boundstone facies (S-6) have depositional fenestral and diagenetic vuggy porosity (non-touching and touching pores). Dissolution is more prevalent in the lower reservoir as compared to the upper reservoir. Therefore, using the Ahr (2008) classification, the lower reservoir's porosity is classified as Hybrid 1B. Vuggy porosity predominates but fenestral porosity is also common. The limestone reservoirs in the Little Cedar Creek field were not pervasively dolomitized and/or cemented thus preserving various amounts of the original depositional porosity. The genetic porosity classification of Ahr (2008) requires the use of pore throats and pore geometry instead of facies, however, facies governs the porosity in Little Cedar Creek field. Diagenesis was facies selective in Little Cedar Creek field (Ridgeway, 2010); therefore, facies identification can be used to delineate the reservoir type in the field area. A permeability–porosity crossplot based on facies is shown in Figure 20. The permeability-porosity plot also shows the ratio of K/ϕ draped over the data. The K/ϕ relationship

defines potential barriers and baffles to flow and flow units (Ahr, 2008; Lafage, 2008). The ratio is an indicator of reservoir quality in terms of flow efficiency of a rock sample (Lafage, 2008). A low ratio indicates possible barriers, or, at least, low-flow rate zones, and the reservoir quality is poor in this case. As can be seen in the Little Cedar Creek field, the upper grainstone reservoir with its moldic pore types has a wide range of porosity values (0- 33 %) with comparable permeabilities (0 to 785 mD). Moreover, the upper reservoir is characterized as a low-flow rate zone because k/ϕ is less than 1. This grainstone reservoir facies grades into lime mudstone and wackestone in the northeast part of the field providing a potential baffle or barrier to flow. The lower microbial boundstone reservoir with its vuggy pore types has higher permeability (up to 7953 mD) even with its lower porosity values (0- 20 %). This is the result of pervasive dissolution of the original fenestral fabric of the microbial boundstone. The porosity- permeability relationship observed in the boundstone reflects a heterogeneous pore network characterized by high tortuosity. With such an interconnected and tortuous pore network, pore throat distribution can differ with the same permeability (Figure 20; Lafage, 2008). The lower reservoir facies associated with a substantial microbial buildups thickness has the highest reservoir quality in the field, because these beds have both lateral and vertical continuity. The vuggy pore system is characterized by pores that are touching and pore throats that are in communication. Barriers and baffles to flow are evident in the lower reservoir in the middle and northeast parts of the field where the buildups are not well developed and lime mudstone is more prevalent.
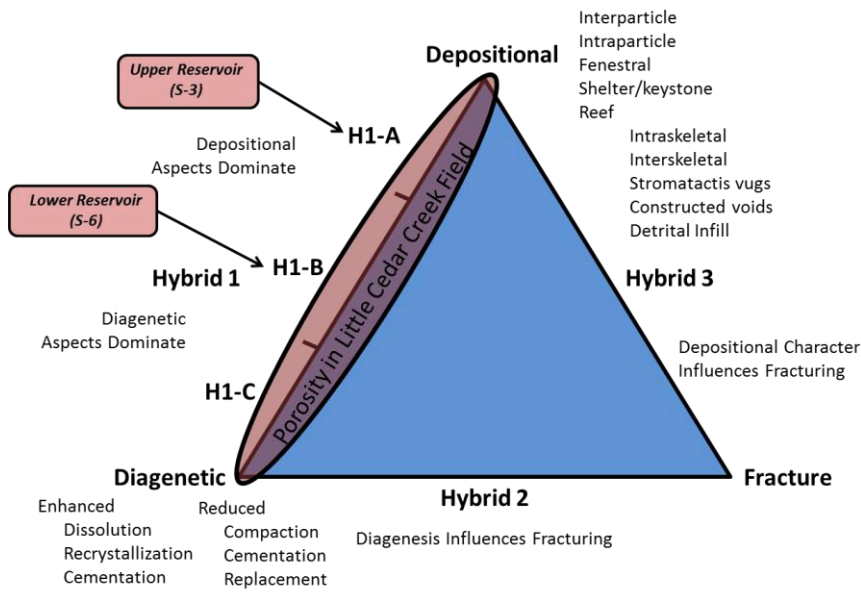
Figure 19. Porosity and pore types in reservoirs at Little Cedar Creek field according to the genetic porosity classification of Ahr (2008). The upper reservoir is classified as Hybrid 1A and the lower reservoir as H1B.
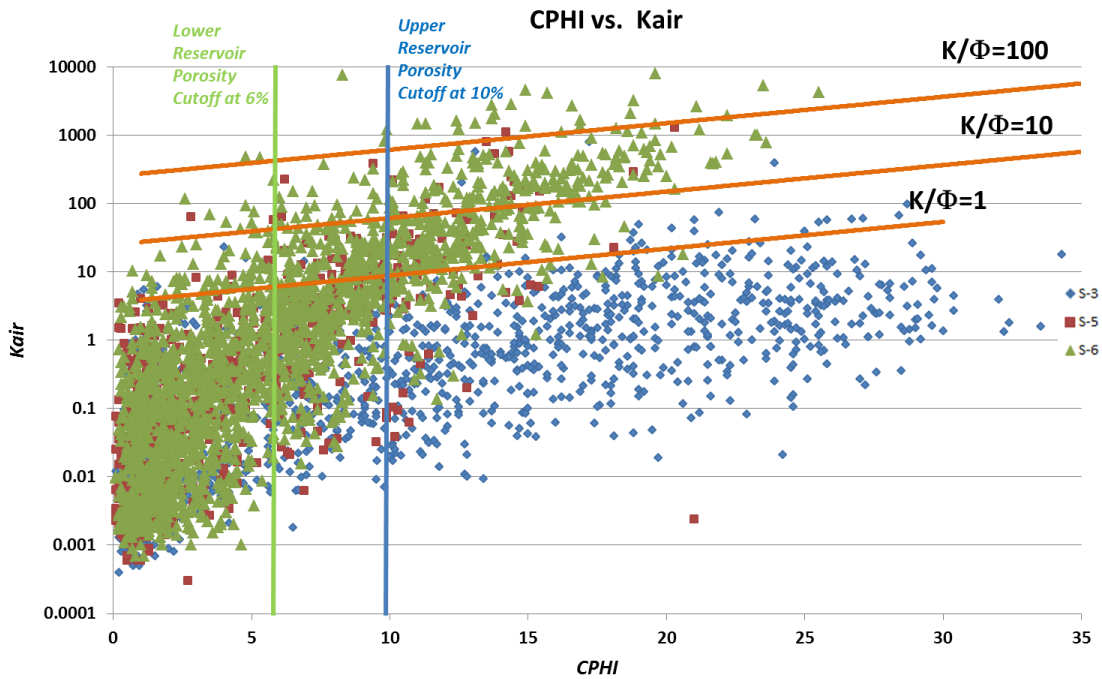
Figure 20. Cross plot of the laboratory measured core porosity (CPHI) vs. laboratory measured air permeability (Kair) for the upper (S-3) and lower (S-5 and S-6) reservoirs in Little Cedar Creek field. Porosity cutoff for the upper reservoir is 10% and 6 % for the lower reservoir.

FORMATION EVALUATION

The objectives of a formation evaluation study in Little Cedar Creek field is to calculate representative petrophysical properties (porosity, water saturation and permeability) of the reservoir rocks in the field and utilize these parameters to construct the 3D reservoir model. The logs most pertinent to the study are gamma ray, resistivity, neutron porosity, density porosity, photoelectric, spontaneous potential and resistivity logs. Available conventional core data analysis (porosity, air permeability and water saturation) was also utilized in this study. Several log interpretation techniques and models are available. Selection of the model depends on variables such as the dominant lithology present in the reservoir rock, type of hydrocarbon in the pore spaces, and the type of data available. Figure 21 shows the workflow followed in log interpretation for the Little Cedar Creek field.

The dominant reservoir lithology was determined using neutron/density crossplots. The two parameters required for the crossplot are the values derived from the neutron porosity and bulk density (ρ_b), both of which are available from the log data. In a limestone matrix, the density-derived porosity and neutron porosity overlay in clean limestone. Neutron/Density crossplots for the Smackover interval are shown in Figures 22, 23 and 24. These crossplots show that the dominant lithology is limestone in the Smackover Formation of the Little Cedar Creek field. Dolomite increases in the S-5 and S7 facies towards the southwest of the field (Permit #13438). However dolomite is absent in the wells to the middle and northeast of the field where the upper reservoir (S-

3) is absent (Permits #14545, 16135). This designates a facies change from packstone to lime mudstone.
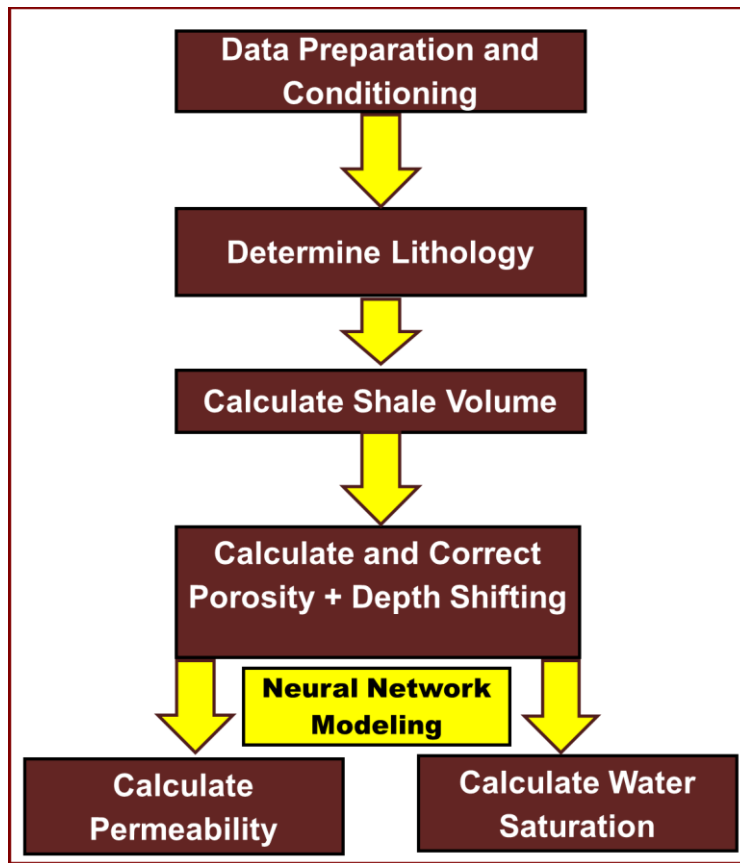
Figure 21. A schematic of the workflow for formation evaluation of the Little Cedar Creek field data.
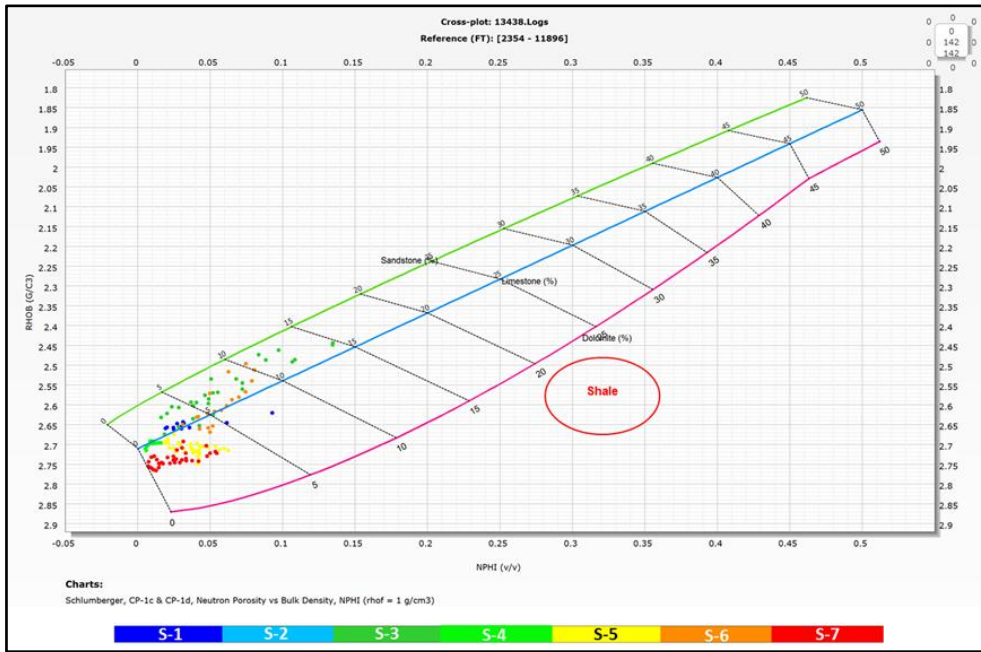
Figure 22. Lithology crossplot of NHPI vs. RHOB of the Smackover facies in permit #13438 in the southwest of the study area. Note the higher dolomite content in the S-5 and S-7 facies.
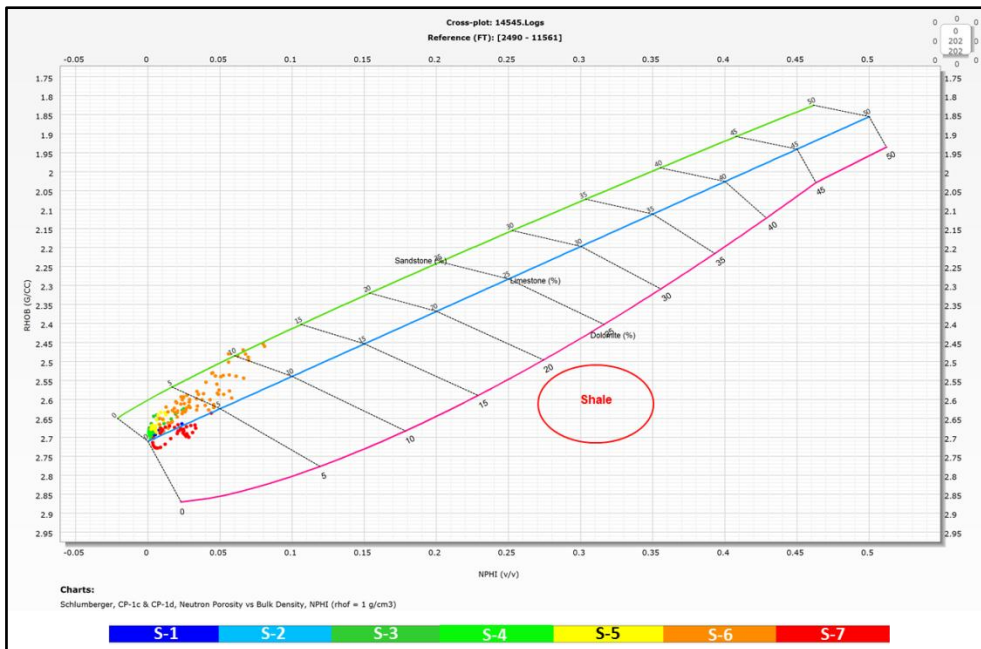
Figure 23. Lithology crossplot of NHPI vs RHOB of the Smackover facies in permit #14545 in the central part of the study area.
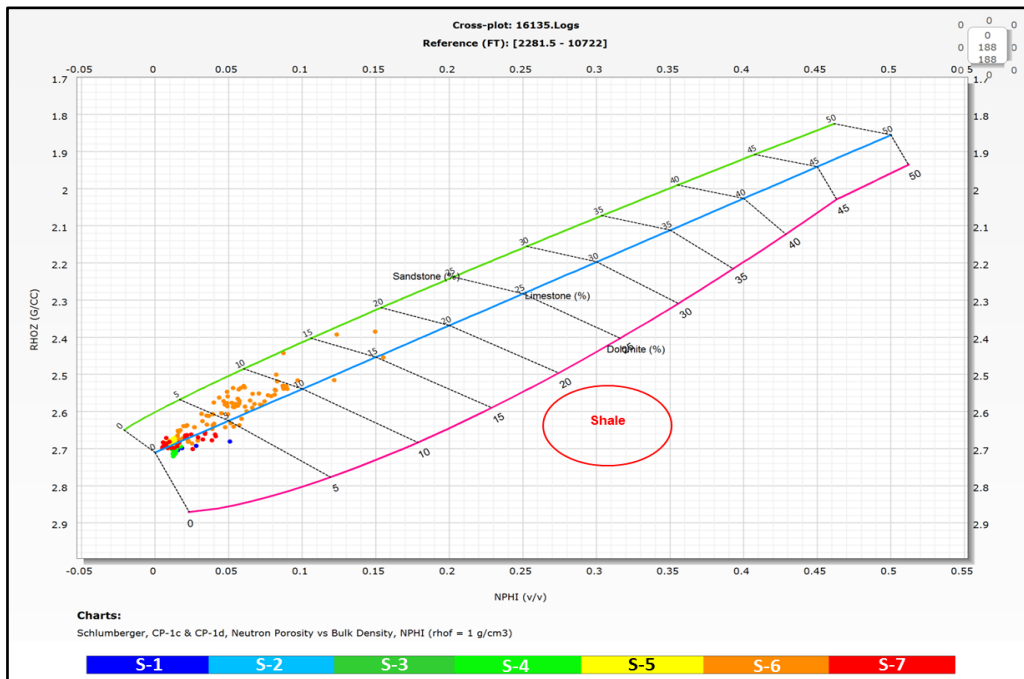
Figure 24. Lithology crossplot of NHPI vs RHOB of the Smackover facies in permit #16135 to the northeast of the study area.

The presence of shale in the formations negatively affects the response of the different logging tools, especially the porosity tools. It also has a high impact on permeability and especially water saturation calculations. When this is the case, the shale volume in these formations should be precisely calculated in order to obtain realistic values. Corrections to the neutron porosity and density-derived porosity are then made by using the calculated value of shale volume. Crossplots (Figures 22, 23 & 24) show that there is no shale in the Smackover Formation of the Little Cedar Creek field. Therefore, there is no need to calculate shale volume for the well logs in the field and no need to correct for log-derived porosity values. Arithmetic average porosity (PHIA) is

thus representative of the correct and effective porosity in the Smackover Formation of Little Cedar Creek field.

The next step is to calculate and derive representative permeability values for the non-cored wells. Core permeability is usually measured in the laboratory using air as a flowing fluid. The available core analysis reports for the Little Cedar Creek field indicate that all permeability was measured by air. Klinkenberg (1941) indicated that permeability measurements made with air as flowing fluid are always greater than liquid permeability. Klinkenberg proposed an equation (Equation 1) for calculating liquid permeability from air permeability.

$$K_g = K_L + c \left[\frac{1}{P_m}\right] \qquad \text{(Equation 1)}$$

K_g = Gas permeability, md

K_L = Liquid permeability, md

P= pressure, psia

C= Constant that varies with permeability (it must be determined for each core plug)

The values necessary to perform the Klinkenberg correction for air permeability were not available for the Little Cedar Creek field. Therefore, we use air permeability (Kair) in this study. The correction would not have a major impact on the permeability values in the Little Cedar Creek field because most of the permeability values are low (Table 1; Halliburton Open Hole Log Interpretation Hand Book, 2004).

Table 1. Table showing general Klinkenberg correction factor applied on air permeability Halliburton Open Hole Log Interpretation Hand Book, 2004).

Air Permeability (md)	Klinkenberg Correction factor	Equivalent Oil Permeability (md)
1000	0.95	950
100	0.88	88
10	0.78	7.8
1	0.68	0.68
0.18	0.66	0.12

In non-cored wells, permeability is most commonly estimated from well logs using either an empirical relationship or some form of linear regression. In sandstone reservoirs, the regression is linear, and a relationship exists between porosity and the logarithm of permeability plotted against each other on crossplots. This is due to the fact the permeability in sandstones is directly related to depositional porosity (mostly intergranular). In carbonates, however, diagenesis, grain size distribution, cementation and pore type distribution alter the relationship, making prediction of permeability complicated. In the last few years, parametric (multi-linear and non-linear models) and non-parametric statistical regressions have been proposed to overcome this problem (Avila et al., 2002; Lee et al., 2002; Mancini et al., 2004; Mathisen et al., 2003). Whereas parametric regression techniques require *a priori* assumptions regarding functional forms, nonparametric approaches (alternating conditional expectations- ACE and artificial neural networks ANN) were successful in overcoming the limitations of the

conventional multi-linear regressions methods (Avila et al., 2002; Lee et al., 2002; Mancini et al., 2004; Mathisen et al., 2003). In addition several approaches have used lithofacies information identified derived from cores to identify hydraulic flow units (HFUs). Other approaches have used pore type characterization and permeability-porosity transforms to predict permeability in complex carbonate reservoirs (Lonoy, 2006). In the Little Cedar Creek field, conventional linear regression techniques fail to accurately predict permeability due to the reservoir heterogeneity and porosity/permeability mismatch (i.e. low permeability in regions exhibiting high porosity and vice versa (Figures 20, 25 and 26).
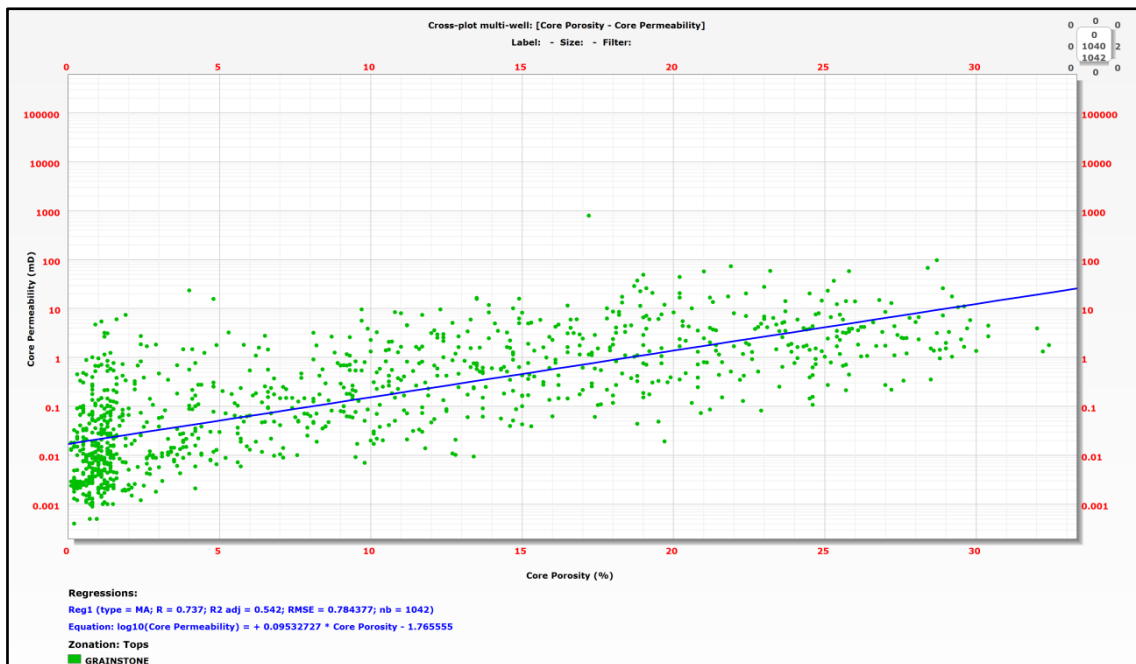
Figure 25. Core porosity vs. core permeability of the grainstone facies (S-3) of the little Cedar Creek field. Note the scattering of the data around the regression line and lack of linear relationship between porosity and permeability.
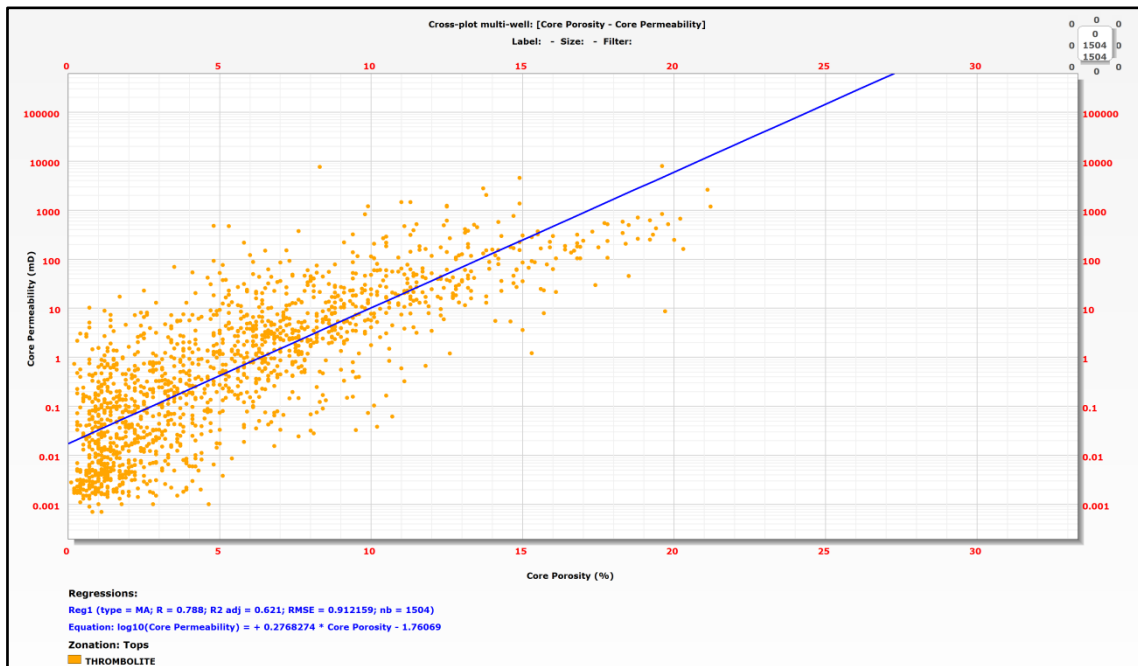
Figure 26. Core porosity vs. core permeability of the microbial (thrombolite) boundstone facies (S-6) of the little Cedar Creek field. Note the scattering of the data around the regression line and lack of linear relationship between porosity and permeability.

Neural Networks

Rogers et al. (1995) proposed ANN to predict permeability in wells in the Smackover in Big Escambia Creek field in southern Alabama. They used back propagation artificial neural networks (BPANNs) to accurately predict permeability using minimal data. The availability of a large amount of core and log data in Little Cedar Creek field makes the use of ANN a good approach for permeability estimation. A neural network can be described as "massively parallel-distributed processor made up of simple processing units called neurons" (Bhatt, 2002). These neurons have a natural tendency for storing experiential knowledge and making it available for use (Bhatt, 2002). Neural networks are applied in a wide variety of fields to solve problems such as

classification, feature extraction, diagnosis, function approximation and optimization

(Bhatt, 2002). They are superior to other methods under the conditions that, 1) the data

on which a conclusion is based is "fuzzy", 2) the patterns important to the required

decision are subtle or deeply hidden, 3) the data has significant unpredictable non-

linearity and 4) the data are chaotic (in the mathematical sense). Most of the above apply

in our case. In this study, we use the multilayer perception (MLP) networks (a variety of

BPANN). The MLPs are currently the most widely used neural networks, and they are

characterized by their ability to classify patterns having nonlinearly separable boundaries

(Bhatt, 2002). The MLP approach is an example of supervised learning that is carried

out through back propagation. The operation consists of an input layer, an internal layer

of hidden neurons and an output layer (Figure 26). The network is provided with

training and validation datasets of known inputs and outputs. In the learning phase,

random weights are applied to the input variables in the hidden layer and the network is

adjusted to minimize the convergence error (root mean square error) with the validation

dataset and the convergence error with the training dataset (Figure 27). Once the

network has finished learning, it starts the training process where the weight values of

the middle hidden layer(s) are adjusted by comparing the network's results to the desired

outputs, and updating the weight values by back propagation to produce better outputs

(Bhatt, 2002; Roger et al., 1995). This process is iterative. However, some

considerations need to be applied so that the network is not over trained. The optimum

output is obtained when the convergence error on both the validation dataset and the

training dataset is minimal (Figure 26). The advantage of using MLP is its ability to

solve problems stochastically and the nonlinear relationship it generates between inputs

and outputs. Moreover, it does not require any *a priori* assumption or relationship in the

data to be made.
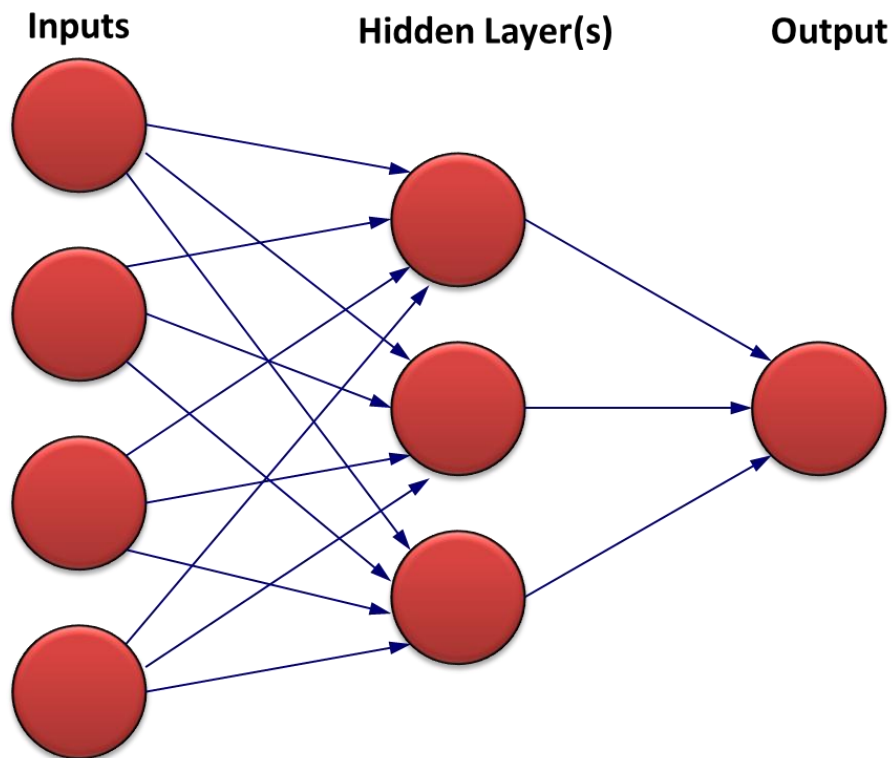
Figure 27. Schematic diagram of a neural network.
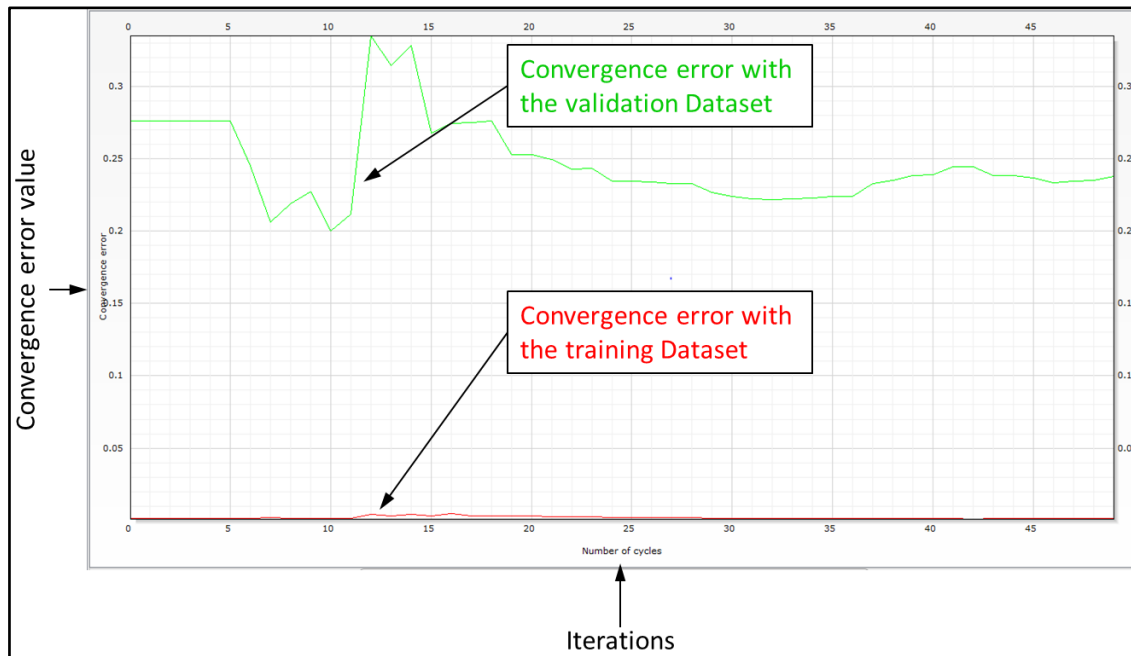
Figure 28. A graph of the results of neural network convergence error when predicting permeability and water saturation from well logs in Little Cedar Creek field.

Permeability Prediction

To predict permeability from well logs in the Little Cedar Creek field, cored wells are used to construct training and validation datasets (Figure 27). Available well logs of gamma ray (GR), deep resistivity (ILD or HDRS), average porosity (PHIA), spontaneous potential (SP) and photoelectric effect (PE) are used as the input variables. However, any of the input variables could be omitted when the log curve does not reflect the unique pattern observed in the reservoirs and surrounding facies. The optimal number of hidden layers of a permeability neural network should be confined to the range 8-12, which would keep the variance and bias at their minimum (Bhatt, 2002). Moreover the optimal number of training patterns should be in excess of 100, to ensure negligible errors in case of data with moderate noise (Bhatt, 2002).

In Little Cedar Creek field, we used 10 hidden layers, and we iterated the process until the minimum value of convergence was obtained (Figure 27). The modeled (output) permeability is shown in Figure 28. The output matches the core data very well keeping in mind that there will never be a perfect match due to errors in original data that would have resulted from measurement conditions, resolution, spatial sampling, and anisotropy (Bhatt, 2002). The availability of the core data for many wells in the field allows us to reconstruct the permeability log in the cored interval using the original core data while predicting the permeability values in the non-cored interval. This process reduces the uncertainty associated with the neural network prediction and allows for improved modeling of permeability in the field (Figure 29). The modeled (predicted) permeability can then be used as a training/validation data set for non-cored wells. In total, 80 wells were used where the level of confidence in predicting permeability using ANN is high (Appendix 1). Average permeability maps of the upper (S-3) and lower (S-6) reservoirs are shown in Figures 30 and 31.
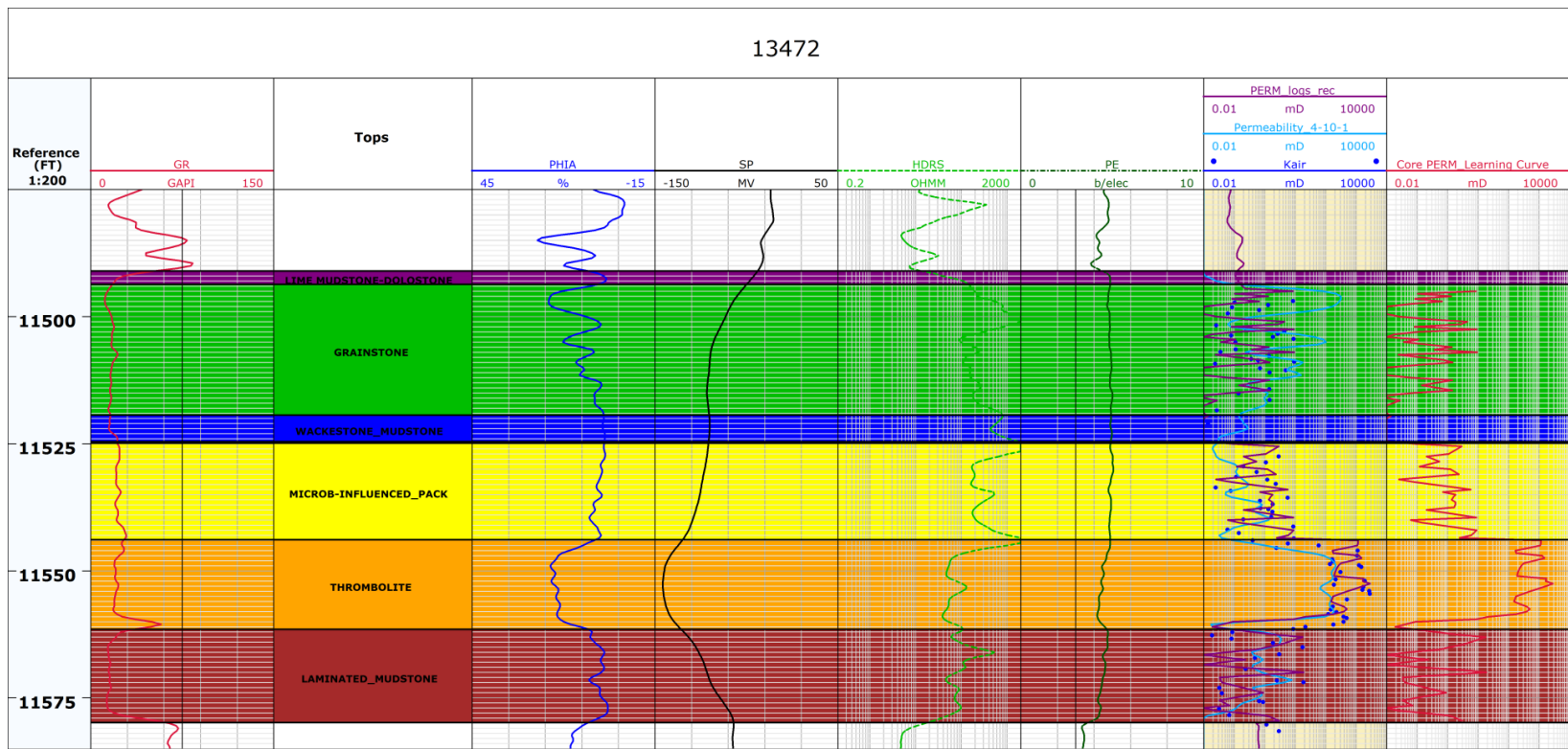
Figure 29. A layout of well logs used to predict permeability in permit #13472 of the study area. Kair log is the core permeability log, permeability_4_10_1 is predicted permeability log, PERM_logs_rec is the reconstructed permeability log.

Figure 30. Average permeability map of the grainstone facies (S-3) constructed from neural network predicted logs.
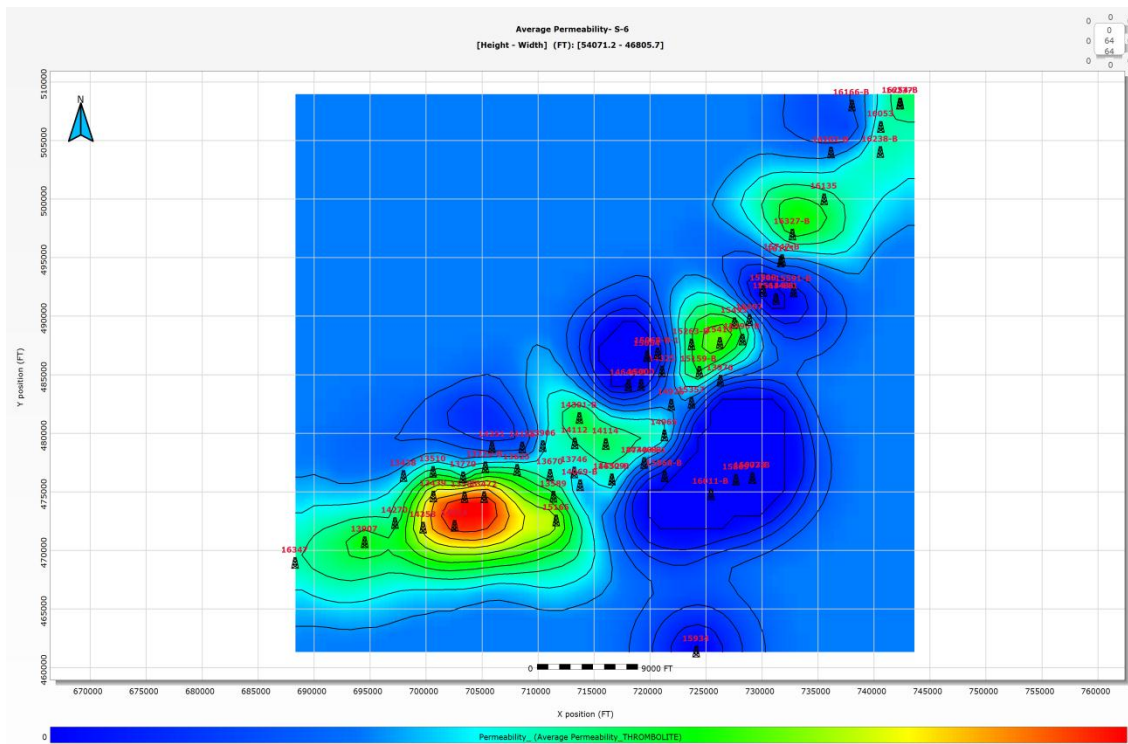
Figure 31. Average permeability map of the microbial (thrombolite) boundstone facies (S-6) constructed from neural network predicted logs.

Water Saturation Prediction

       The absence of any special core analysis data (SCAL) and the heterogeneity of the reservoir in Little Cedar Creek field decrease the level of confidence in predicting the electrical parameters (a, m, n) of the reservoirs. Thus applying any of the available water saturation models (Archie, waxman-smits, etc.) to derive water saturation in Little Cedar Creek field without any measured data would be a high risk exercise and associated with much uncertainty. Therefore, we utilize the MLP approach again to predict and model water saturation in the field. The input logs used in this case are: gamma ray (GR), deep resistivity (ILD or HDRS), average porosity (PHIA), and apparent water resistivity (Rwa) provided by the vendor. The apparent water resistivity

has a unique signature in the reservoirs that can be used to properly train and model the

water saturation (Figure 31).
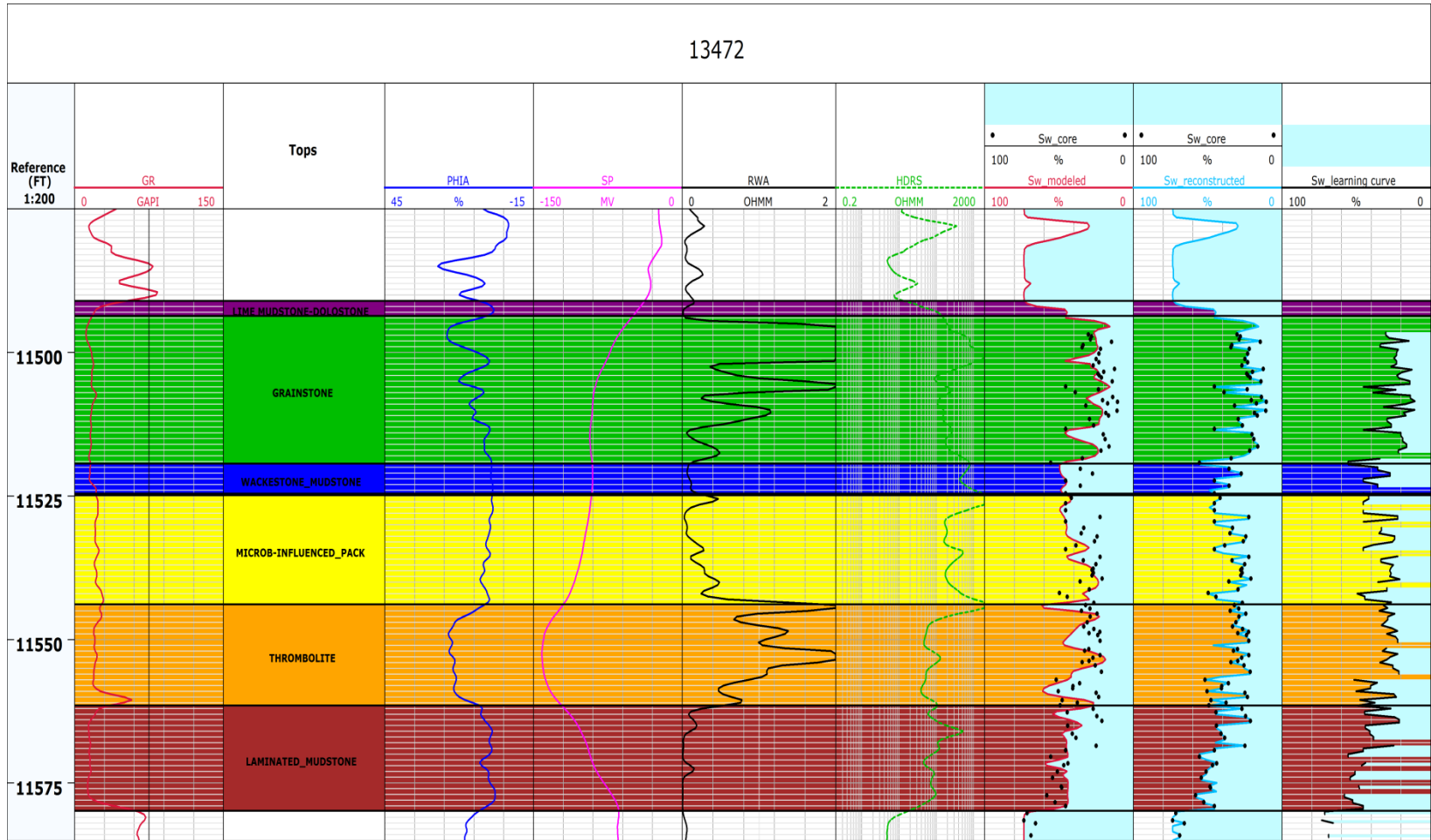
Figure 32. A layout of well logs used to predict water saturation in well permit 13472 of the study area. Sw_core log is the core water saturation log, Sw_modeled is predicted log, Sw_reconstructed is the reconstructed log.

3-D GEOLOGIC MODELING

The purpose of building a 3-D geologic model is to provide a static framework for strategic reservoir wide field development including reservoir simulation and history matching studies. The model incorporates data and interpretations from the core and well logs analysis, stratigraphic and depositional history (Mancini et al., 2008; Ridgway 2010), petrographic analysis (Mancini et al., 2008; Ridgway 2010), and diagenetic and formation evaluation studies. The 3-D stratigraphic and petrophysical grid provide an interpretation for the interwell distribution of lithofacies, reservoir-grade rock, porosity, permeability and heterogeneity throughout the field. Geologic 3-D modeling is a cost effective reservoir management tool for making decisions regarding operations in the field.

Stratigraphic Model

Figure 2 shows the boundaries of the Little Cedar Creek field as identified by the State Oil and Gas Board of Alabama. The boundary of the field to the west is the discovery well (permit # 10560) which is marginally productive and dry hole permit #16347. To the east and north, the field is bounded by dry holes (Permits # 16067, 16366-B-1, 15544, 10952, 14600-B, 16174 and 16122-B) that are marked by substantial facies change. The recently discovered Brooklyn Field is adjacent to the southern border of Little Cedar Creek field. Brooklyn field is characterized by absence of the clear "thrombolitic" signature that is diagnostic of the microbial boundstone reservoir in Little

Cedar Creek field (Figure 33). On wells logs from wells located in the southeast part of

the Little Cedar Creek field, the "thrombolitic" signature is also not evident. In addition,

wells (Permit #14216 and 15416) are dry holes. The Little Cedar Creek field is distinct

from other fields in the area by its two separate reservoirs, upper nearshore high energy

shoal grainstone reservoir and lower microbial (thrombolite) boundstone reservoir.

Therefore, the geological boundary of the Little Cedar Creek field was redrawn at the

limits of the two dry holes (Permit #14216 and 15416) (Figure 34). This boundary will

be used to construct the geological 3D model in this study.
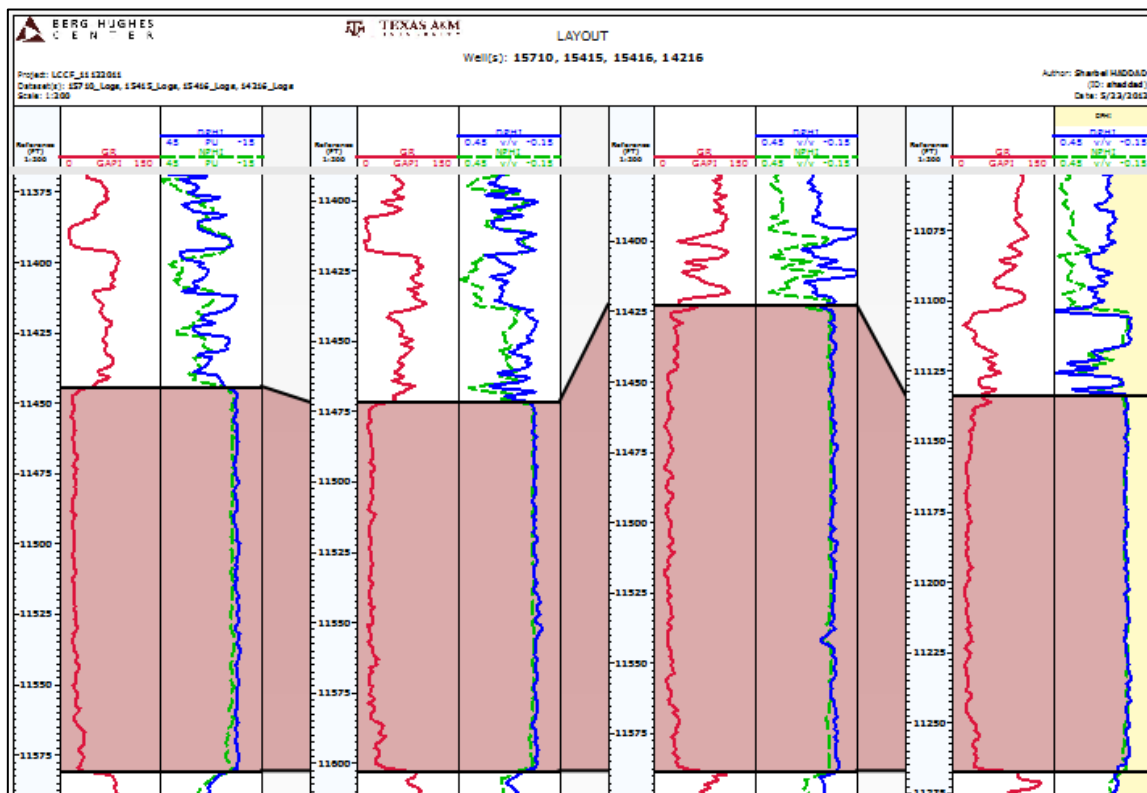
Figure 33. A cross section in the southeast part of the Little Cedar Creek field. The "thrombolitic" signature in dry holes (Permit #14216 and 15416) is not evident.

To construct the stratigraphic grid, well locations, well surveys, and well tops were imported into Paradigm's SKUA$^©$ modeling package. The stratigraphic and sedimentologic information obtained from the reservoir characterization studies (core, well-log, and thin section analysis; cross sections and isopach maps) are incorporated into the model. The final grid is shown in Figure 35. The grid incorporated 6 subhorizontal stratigraphic horizons and excluded the S-2 facies surface, which is observed in only two wells (Table 2). Vertical layering was conformable between facies, except for the S-3 facies that was set as baselap to truncate it in the northeast part of the field where it is absent. The vertical number of cells and vertical cell thickness are shown in Table 2. Horizontally, the cells widths are 250x250 feet. The model was constructed with a 65$^°$ northeast trend to reflect the paleo-depositional strike of the field and the depositional pattern observed in the isopach and permeability maps of the S-3 and S-6 facies (Figures 15, 16, 30 and 31).

Table 2. Parameters used to build the 3D stratigraphic grid of the Little Cedar Creek field.

	Stratigraphic Unit	Layering	Build	Vertical Number of cells	Vertical Cell thickness
Top of Smackover	(S-1)	Conformable	Yes	10	2
	(S-3)	Baselap	Yes	27	2
	(S-4)	Conformable	Yes	10	7
	(S-5)	Conformable	Yes	12	2
	(S-6)	Conformable	Yes	25	2
	(S-7)	Conformable	Yes	10	5.5
Base of Smackover	Norphlet	Conformable	No		

Figure 34. Map (top view) of the new boundary of the Little Cedar Creek field used to construct the 3D Geocellular grid.
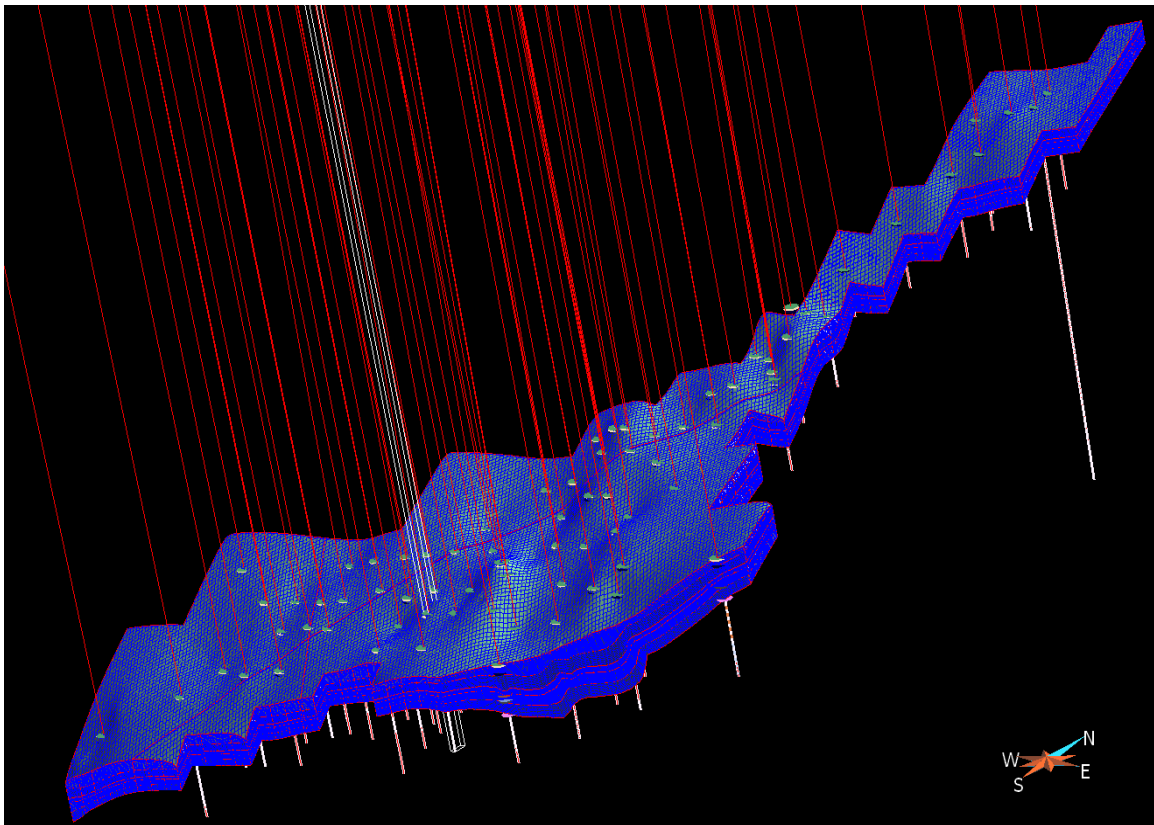
Figure 35. The constructed 3D geoscullar grid of the study area showing the wells and well tops (20 times vertical exaggeration).

Facies Model

Truncated Gaussian simulation is used to model the facies in the Little Cedar Creek field. Pixel-based simulation (Sequential Indicator Simulation - SIS and Truncated Gaussian Simulation- TGS) methods are better to use in modeling carbonate environments. The object-based modeling is not suitable for our area (carbonate environment) where post-depositional processes (dissolution, re-precipitation, dolomitization, fracturing, etc.) dominate and therefore altering the depositional patterns or geometry/shape. The primary data input to run a Truncated Gaussian Simulation are: a) upscaled facies data blocked into the grid from facies logs, b) the order the facies in

the model, c) one variogram that is used for all facies, and the global fraction/ trend of

each facies. Secondary data input include vertical facies proportion curves (VPCs) and

3D, 2D, or 1D trend maps if available. In Little Cedar Creek field the facies logs are

generated from the facies that were picked on each well (S-1 to S-7) and observed from

core studies where each facies is coded a number to create the discrete facies logs

(Figure 35). An experimental variogram is then computed from facies logs, and then

fitted the variogram model to obtain horizontal and vertical ranges of the facies. We use

a spherical isotropic variogram model with 5300 feet in R1 (maximum) and R2

(minimum) ranges and 21 feet for the vertical range. No trend was used in the variogram

but the horizontal variogram model was fitted to the experimental in the 0, 60, 90 and

120° directions. Vertical facies proportion curves are obtained from data analysis and

used to constrain the model (Figure 36). In general, wells are drilled in areas with the

greatest probability of high production (cores are taken preferentially from good quality

reservoir rock). Such data collection practices lead to the best economics and the greatest

number of data in portions of the study area that are the most important economically.

Therefore, subsequent bias oversampling occurs in some areas and under sampling is

evident in other areas. During the data analysis, we use de-clustering techniques to

remove sampling bias and establish unbiased statistics. Ten simulations were then

performed using the Truncated Gaussian simulation technique to build the facies model

(Figure 37, 38 and 39).
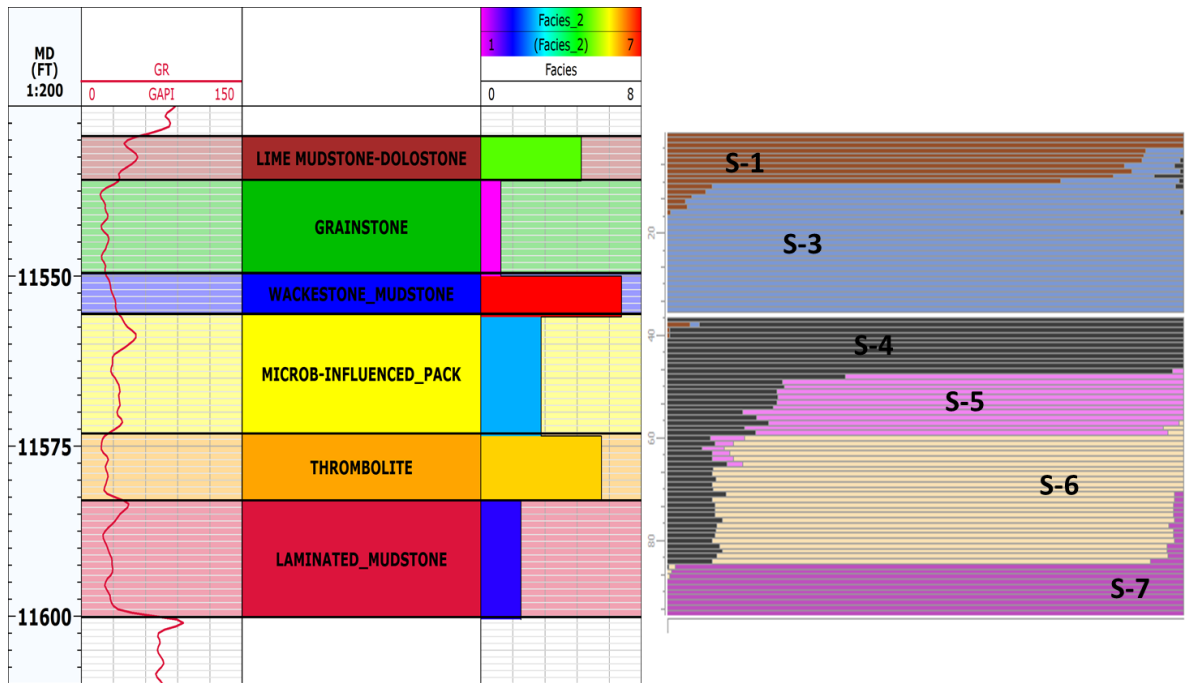
Figure 36. Facies logs and vertical proportional curves in the Little Cedar Creek field.
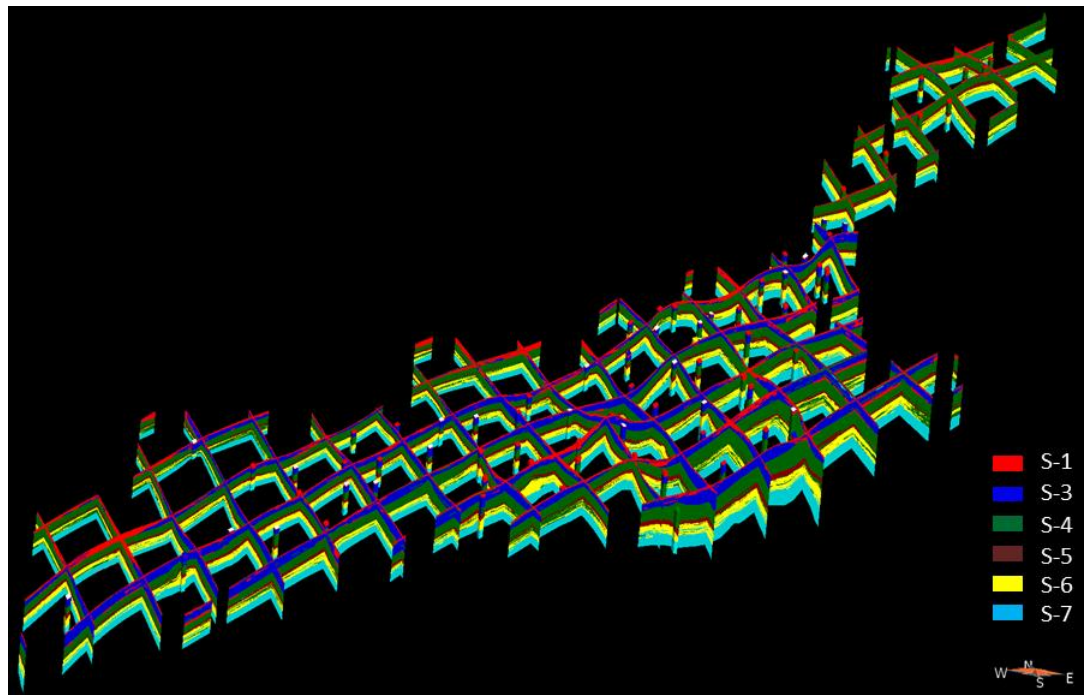
Figure 37. Fence diagram of the 3D model showing the facies distribution in 3D. Diagram constructed every 13 grid section in I and J (x and y) directions (20 times vertical exaggeration).
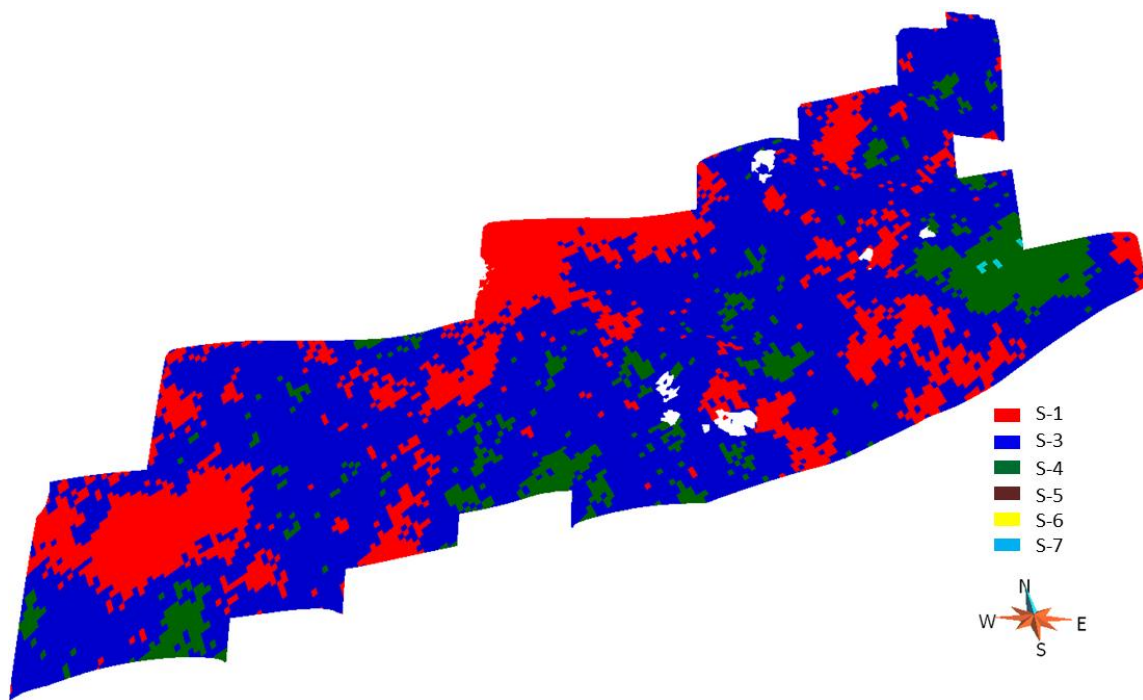
Figure 38. A depth slice on top of S-3 facies showing the distribution of facies (20 times vertical exaggeration).
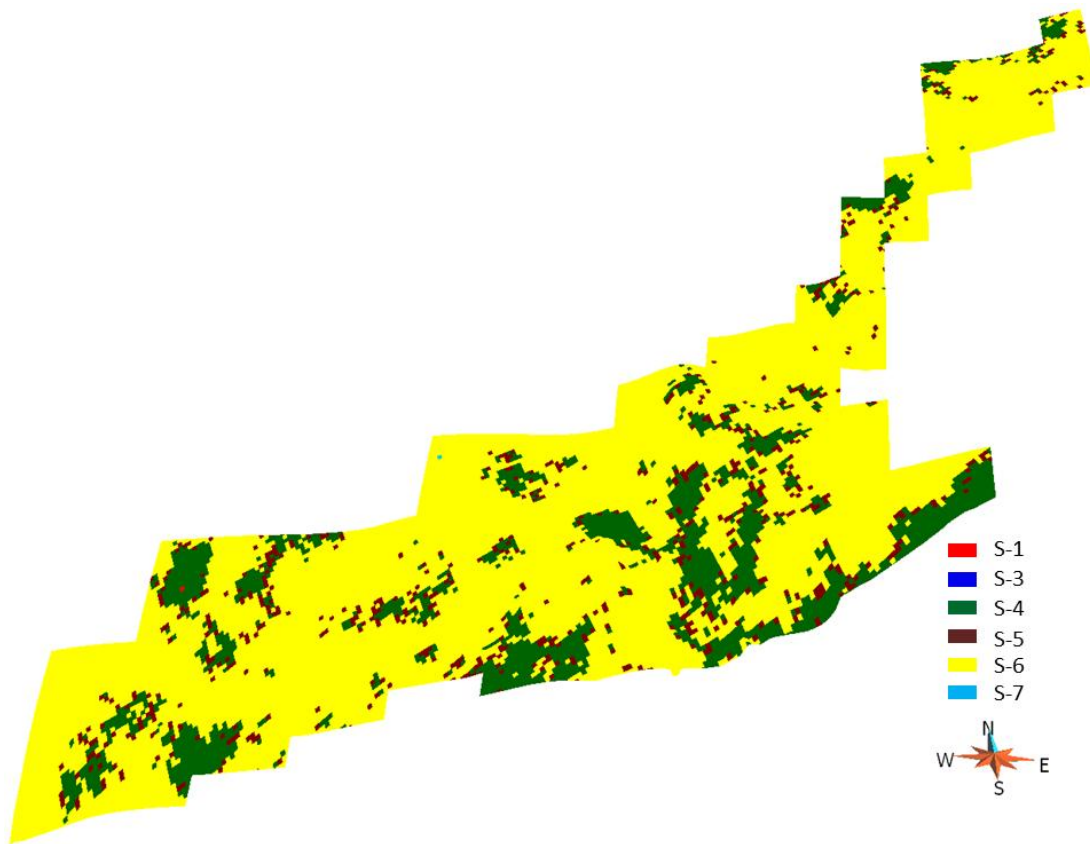
Figure 39. A depth slice on top of S-6 showing the distribution of facies (20 times vertical exaggeration).

Porosity Model

In the Little Cedar Creek field, the facies govern the porosity distribution, and

diagenesis is facies selective (Ridgway, 2010). Thus, the porosity model in the Little

Cedar Creek field should be facies constrained. We use Sequential Gaussian Simulation

(SGS) to model the porosity in the area of study. The SGS technique is applied to

interpolate data between wells and to obtain multiple realizations. One variogram is

required for the SGS simulations. The experimental variogram displays cyclicity in the

vertical direction. The cyclicity is a product of microbial buildup development and

resulting heterogeneity in the field. We use a spherical isotropic variogram model with 7962 feet in R1 (maximum) range and R2 (minimum) range and 25 feet for the vertical range. No trend was used in the variogram but the horizontal variogram model was fitted to the experimental in the 0, 60, 90 and 120° directions. Average porosity logs (PHIA) from wells are blocked to the grid cells using arithmetic mean, and 10 simulations per each facies are then performed using the SGS technique to obtain the porosity model (Figures 40 and 41).
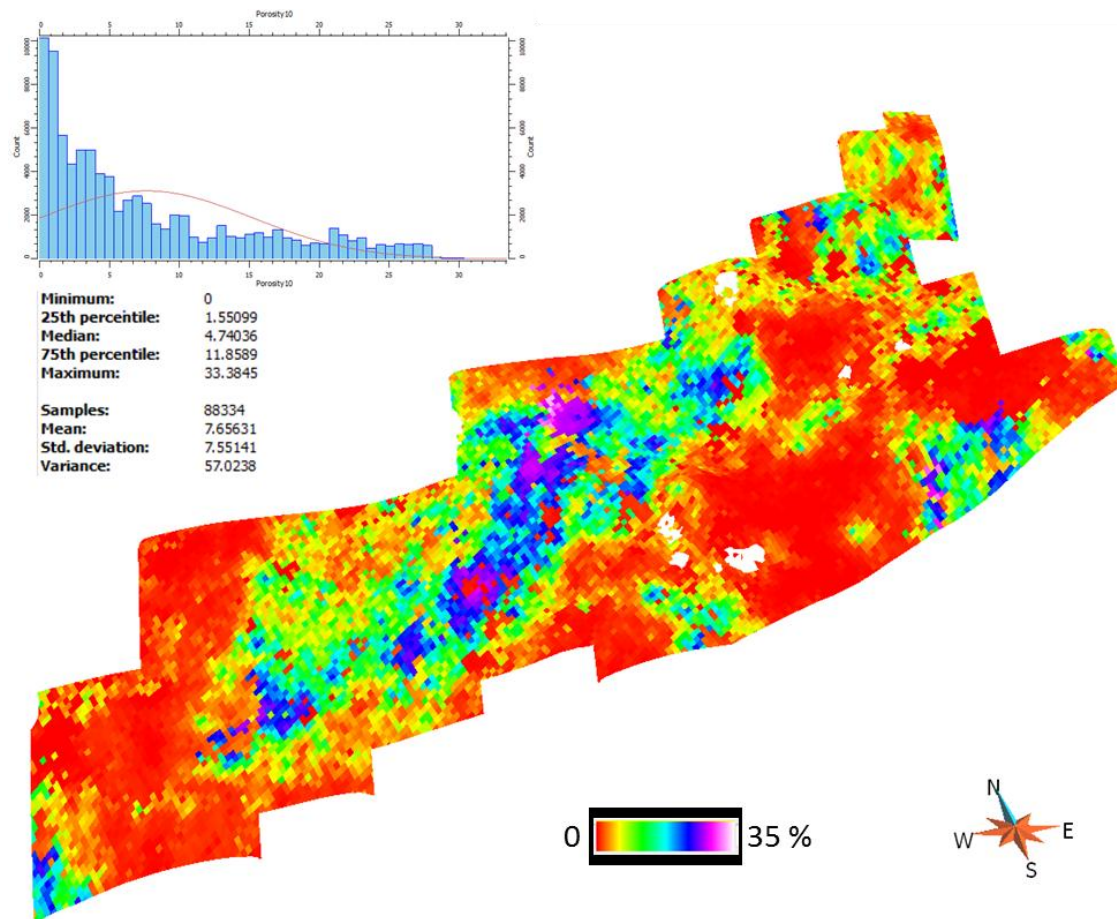
Figure 40 A depth slice on top of S-3 facies showing porosity distribution in the upper reservoir (20 times vertical exaggeration).
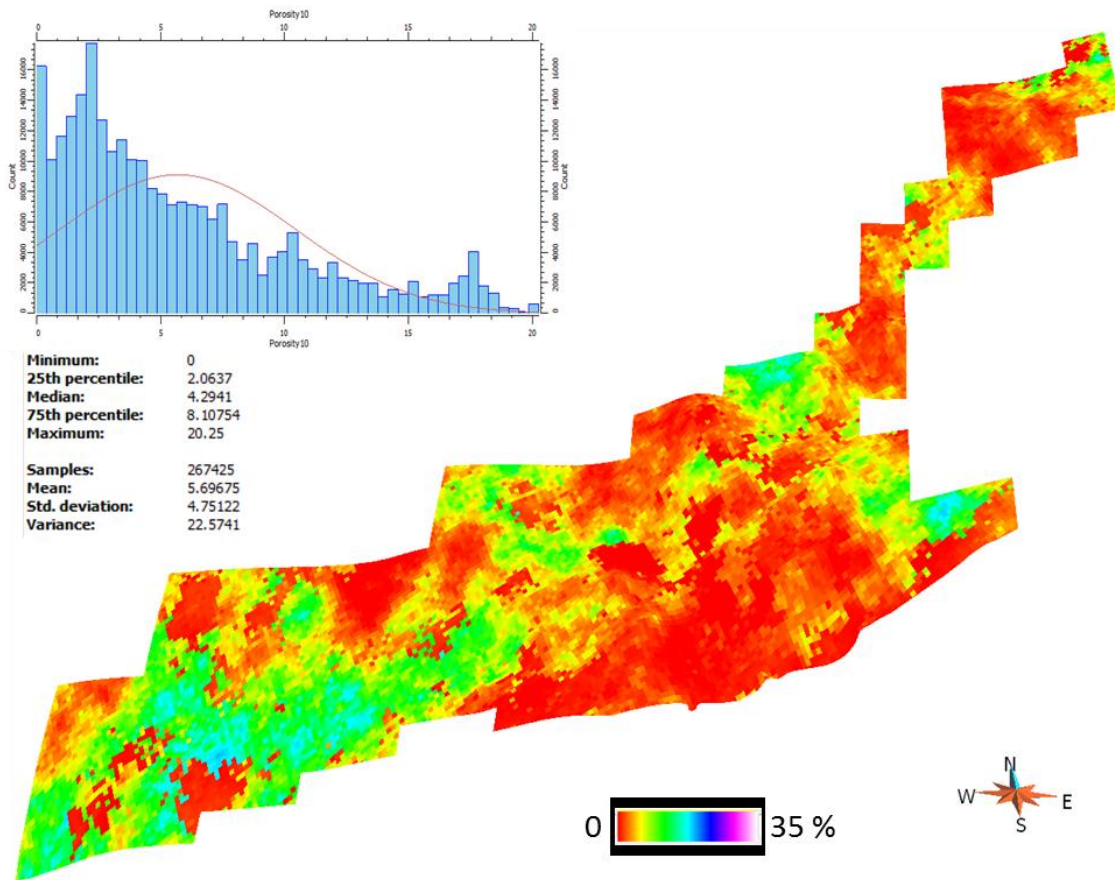
Figure 41. A depth slice on top of S-6 facies showing porosity distribution in the lower reservoir (20 times vertical exaggeration).

Permeability Model

Permeability is a difficult reservoir parameter to model as it is highly variable and is characterized by extreme values. Extreme low values in a facies potentially result in a baffle or barrier to flow while and extreme high values in a facies have the potential to facilitate flow and serve as a flow conduit. Also important are the direction of flow and local pressure conditions. The permeability distribution often has a highly skewed

histogram, and thus cannot be linearly averaged. Typically, the logarithm of permeability is used because of the skewed nature and approximately log normal character of many permeability histograms. Moreover, the models of permeability must also account for any relationship with porosity. SGS with collocated cokriging is a technique, which can account for a statistical relation between two variables. The statistical relation is a simple linear correlation between porosity and log permeability. In Little Cedar Creek field, the linear relationship between porosity and permeability is obtained by plotting the predicted permeability log versus core porosity on a crossplot. However, correlation values should be used with caution in this case due to the highly variable porosity- permeability relationship in a heterogeneous interconnected pore system network characterized by a tortuous flow pathway system as is the case with the reservoirs at Little Cedar Creek field. Geometric and power averaging methods are recommended to upscale (block) permeability from wells into the grid. We use geometric mean in our study as this method is sensitive to low values of permeability and would subsequently honor flow units.

We use a SGS with collocated cokriging to generate a permeability model (10 simulations/ realizations) that honors the modeled variogram, has the observed correlation with the porosity, and matches the permeability data from wells (Figures 42 and 43).
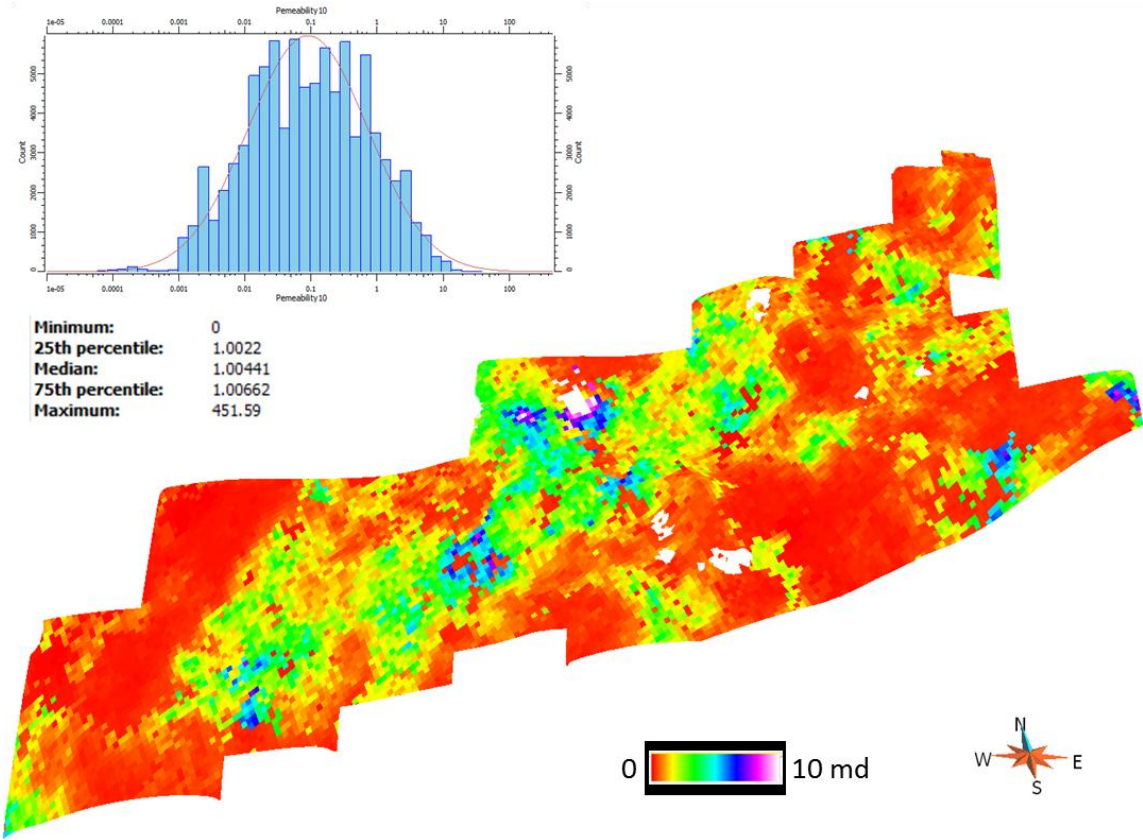
Figure 42. A depth slice on top of S-3 facies showing permeability distribution in the upper reservoir (20 times vertical exaggeration).
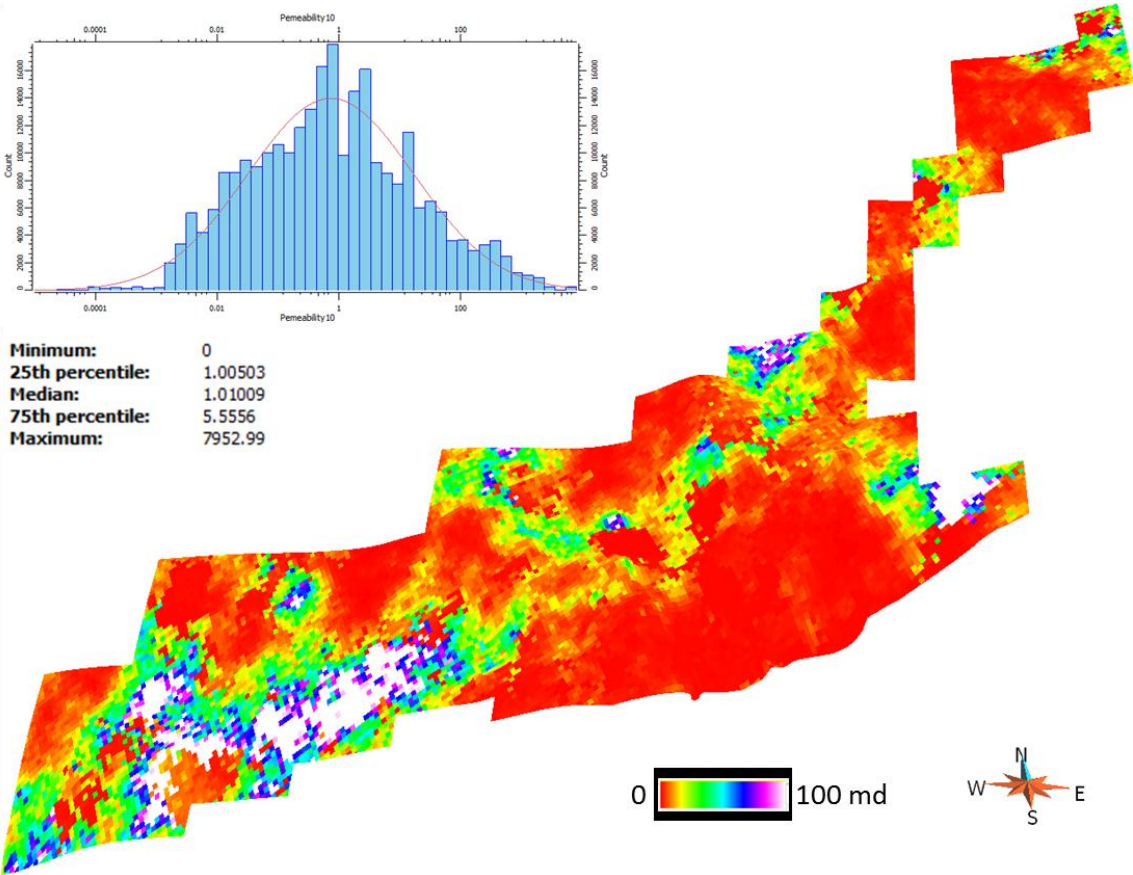
Figure 43 A depth slice on top of S-6 facies showing permeability distribution in the lower reservoir (20 times vertical exaggeration).

RESULTS AND DISCUSSION

The 3D geologic modeling conducted in this study confirms that the upper (high energy shoal grainstone and packstone facies, S-3) and lower (microbially influenced packstone facies, S-5 and microbial (thrombolite) boundstone facies, S-6) reservoirs in the Litte Cedar Creek field are separate and are potentially not in flow communication vertically or laterally. The modeling also shows that both reservoirs are heterogeneous and potential flow baffles and barriers occur in these reservoirs. The lime mudstone facies (S-4) serves as a vertical barrier between (S-3) and (S-5 and S-6), and the lime mudstone and dolomudstone to wackestone facies (S-1, S-4 and S-7) act as lateral barriers to flow for the lower and upper reservoirs. The top seal for the upper reservoir is the S-1 facies and the argillaceous beds of the overlying Haynesville Formation. The top seal for the lower reservoir is the S-4 facies, and the base seal is the S-7 facies.

The geologic modeling confirms that the upper reservoir (high energy shoal grainstone and packstone) is absent in the northeast part of the field. The absence of the upper reservoir in this part of the field was attributed to a facies change (Mancini, 2008; and Ridgway, 2010). They interpreted this area as being dominated by a low-energy more restricted lagoonal setting. The Conecuh Ridge and Pensacola Arch affected Smackover deposition in this embayment area. The predominance of lime mudstone facies in the upper embayment area as opposed to high energy shoal grainstone and packstone in the embayment proper resulted in a potential barrier or baffle to flow. The

increase in lime mudstone in the northeast part of the field produced a low-flow rate zone where K/ϕ is less than 1 (Figure 19).

This wide distribution and range of porosity values versus permeability values in the upper reservoir, grainstone and packstone facies, is attributed to the bimodal porosity distribution of the pore types, moldic and intergranular/interparticle. Pore systems dominated by interparticle pores generally have higher effective porosity and higher permeability due to the improved connectivity in this pore system. However, pore systems dominated by moldic pores generally have lower effective porosity and lower permeability because the moldic pores are not well connected. Thus, total porosity increases but effective porosity and permeability may not increase. Therefore, we observe relatively higher porosity values but lower permeability values in the upper reservoir. The upper reservoir exhibits the highest porosity and permeability in the central part of the field where this facies is best developed due to environmental conditions, such as paleocurrents, water depths, wave action, wind direction, and bioturbation. These factors produced the southwest- northeast trend for this facies. During deposition of the Smackover Formation, higher energy environments were concentrated in the south, southeast and central parts of the field.

The lower reservoir, microbial (thrombolite) boundstone and overlying microbially influenced packstone facies, is a higher quality reservoir because effective porosity and permeability is generally higher than in the upper reservoir. This is the result of the diagenetic processes of dissolution that acted on the facies during its geologic history. The pore system in this reservoir is dominated by secondary vuggy

pores with some primary fenestral pores that are interconnected. The fenestral and vuggy

pores are touching and in flow communication. However, the combination of both high

and low porosity rocks having high permeabilities results in a heterogeneous and

tortuous pore network. Such a pore system is characterized by a variable pore throat

distribution and sizes but having the same permeability (Figure 19; Lafage, 2008).

The microbial buildups have the highest reservoir quality in the field and their beds

provide good lateral and vertical continuity. The modeling indicates that potential flow

barriers and baffles are evident in the lower reservoir in areas where the well-developed

buildups are absent. Thus, it is important to determine what geologic factors are

controlling buildup development. Typically, in other fields in Alabama the buildups are

associated with paleohighs. In the Little Cedar Creek field area, no substantial paleo

antecedent topography is observed, and only subtle relief occurs on the Norphlet surface.

These subtle Norphlet topographic highs may have acted to promote microbial colony

development and growth in tranquil, restricted conditions in an arid environment

according to Ridgway (2010). No subtle features are evident either on the structure maps

drawn on top of the Norphlet and Smackover formations or in the 3D model (Figures 17

and 18). However, subtle changes in elevation are observed in the model. These changes

are up to 2 m (6.5 feet; Figure 37). This implies that antecedent topography on the

Norphlet Formation had little influence on development of the thrombolites. However,

the acquisition of 3-D seismic data in the field area may result in the detection of

paleohighs associated with crystalline basement structure. Moreover, the thrombolite

development seems to be due to a combination of environmental conditions as discussed

by Mancini (2008). The beds of the microbial facies have a southwest northeast trend suggesting that the circulation of water during their development and diagenesis followed a southwest-northeast direction.

The 3D modeling results indicate compartmentalization in the upper and lower reservoirs. Average permeability maps generated from wells logs (Figures 30 and 31) confirm a southwest- northeast trend in permeability the lower and upper reservoirs. However, high permeability areas are localized and are separated by low permeability areas representing potential flow baffles or barriers. This discontinuous distribution in high permeability suggests compartmentalization in the reservoirs. Major high permeability zones in the upper reservoir are concentrated in the southwest and central parts of the field where the high energy nearshore grainstone and packstone facies are well developed. Enhanced porosity could have attributed to the increase in permeability in these zones. Moreover, the increase in lime mudstone facies to the northeast results in potential permeability barriers and/or absence of reservoir grade rocks. In the lower reservoir, a trend in compartmentalization is also seen in a southwest- northeast direction. The main high permeability zones are distributed in three major areas in the southwest, central and northeast parts of the field. This trend indicates that the main flow units are potentially closely related to the orientation and development of the boundstone beds of the microbial buildups. Enhanced depositional porosity through the creation of vuggy pores resulted in improved connectivity and increased permeability in the boundstone facies.

The results from the 3D geologic modeling can be used in formulating a strategic reservoir-wide management and development plan. For example, the drilling locations for infill drilling and field extension can be identified using the knowledge gained from the 3D geologic model. The southwest-northeast trend observed in the Little Cedar Creek field is related not only to paleocurrent direction and subtle differences in relief but also to the encroachment of meteoric water that has affected the relation between reservoir porosity and permeability. Production data from the Alabama State Oil and Gas Board show that the most productive wells are located in the northeast and central parts of the field (Permit #13625, 16223-B, 16135, 14545, 16293, and 16091). The lateral extent of these major flow and hydrocarbon productive units is important in the design of a cost effective infill drilling and injection program for the field. Reservoir orientation and extent is important in extending the reservoir limits in the field area. Both reservoirs occur in the central part of the field, but the upper reservoir is absent to the northeast. The lower and upper reservoirs are both productive in the southern part of the field suggesting a potential to extend the field limit to the south and an effective recovery plan in the center of the field where the flow units have good lateral and vertical extent.

CONCLUSION

The integration of reservoir characterization, formation evaluation, and 3D geologic modeling in Little Cedar Creek field has shown that the reservoirs of the field are potentially not in flow communication with each other and are compartmentalized. The hydrocarbon-productive reservoirs are the microbial and nearshore high energy shoal carbonate facies of the Upper Smackover Formation separated vertically by a subtidal lime mudstone facies that acts as vertical seal. Lime mudstone and dolomudstone to wackestone units serve as top, lateral and base seals for these reservoirs. The facies were deposited in an inner carbonate ramp setting in shallow subtidal water depths near the Upper Jurassic (Oxfordian) Smackover paleoshoreline in the eastern Gulf coastal plain of the United States.

The integrated approach of the current study has shown that the potentially major flow units of the upper reservoir are localized in the southwest and central parts of the field. Updip and to the northeast of the field the upper reservoir is absent. The area of significant microbial buildup development constitutes potentially the major flow units for the lower microbial (thrombolite) boundstone reservoir. The highest permeability zones in the lower reservoirs occur in the southwest, central and northeast parts of the field. Further development of the field needs to take into account the various reservoir compartments that are not in communication with each other because the efficiency of enhanced recovery and stimulation plans potentially could only be localized. Therefore,

the implementation of any enhanced recovery projects for the field would be maximized

if based on a thorough knowledge of the reservoir heterogeneity in the field.

REFERENCES

Ahr, W.M., 1973, The carbonate ramp: an alternative to the shelf model: Gulf Coast
Association of Geological Societies Transactions, v. 23, p. 221-225.

Ahr, W. M., 2008. Carbonate Reservoir Geology: College Station, Texas, Wiley and
Sons, 277 p.

Alabama Oil and Gas Board, 2009, An Overview of the Little Cedar Creek Field
Development,

[http://www.gsa.state.al.us/documents/misc_ogb/lcc_overview.pdf], 06/01/2012.

Avila, J.C., Archer, R.A., Mancini, E.A., and Blasingame T.A., 2002, A petrophysics
and reservoir performance-based reservoir characterization of the Womack Hill
(Smackover) field (Alabama): SPE 77758, Annual SPE Technical Conference
and Exhibition, San Antonio, Texas.

Bhatt, A., 2002, Reservoir properties from well logs using neural networks: Ph.D.
dissertation, Norwegian University of Science and Technology, Trondheim,
Norway, 173 p.

Baria, L.R., Stoudt, D.L., P.M. Harris, and P.D. Crevello, 1982, Upper Jurassic reefs of
Smackover Formation, United States Gulf Coast: American Association of
Petroleum Geologists Bulletin, v. 66, p. 1449-1482.

Benson, D.J., 1982, Late-stage moldic porosity in the Smackover Formation of
Alabama: Geological Society of America Abstracts with Programs, v. 14, no. 1-
2, p. 4.

Benson, D. J., 1988, Depositional history of the Smackover Formation in southwest
Alabama: Gulf Coast Association of Geological Societies Transactions, v. 38, p.
197–205.

Benson, D.J., 1996, Classification of heterogeneities in Smackover reservoirs, southwest
Alabama: Geological Society of America Abstracts with Programs, v. 28, no. 2,
p. 3.

Bradford, C. A., 1984, Transgressive-regressive carbonate facies of the Smackover
Formation, Escambia County, Alabama, in Ventress, W. P. S., Bebout, D. G.,
Perkins, B. F., and Moore, C. H., eds., The Jurassic of the Gulf rim: Gulf Coast
Section, Society of Economic Paleontologists and Mineralogists p. 27-29.

Crevello, P.D., and Harris, P.M., 1984, Depositional models in Jurassic reefal buildups,
in Ventress, W.P.S., Bebout, D.G., Perkins, B.F., and Moore, C.H., eds., The
Jurassic of the Gulf Rim: Society of Economic Paleontologists and
Mineralogists, Gulf Coast Section, Proceedings of the Third Annual Research
Conference, p. 57-102.

Dobson, L. M., 1990, Seismic stratigraphy and geologic history of Jurassic rocks,
northeastern Gulf of Mexico: Master's thesis, University of Texas at Austin,
Austin, Texas, 165 p.

Dobson, L.M., and R.T. Buffler, 1997, Seismic stratigraphy and geologic history of
Jurassic rocks, northeastern Gulf of Mexico: American Association of Petroleum
Geologists Bulletin, v. 81, p. 100-120.

Kopaska-Merkel, D. C., 1998, Jurassic reefs of the Smackover Formation in south Alabama: Geological Survey of Alabama Circular 195, 28 p.

Kopaska-Merkel, D. C., 2002, Jurassic cores from the Mississippi Interior salt basin: Geological Survey ofAlabama Circular 200, 83 p.

LaFage, S., 2008, An Alternative to the Winland R35 Method for determining carbonate reservoir quality: Master's Thesis, Texas A&M University, College Station, Texas, 102 p.

Lee, S. H., Arun, K., and Datta-Gupta, A., 2002, Electrofacies characterization and permeability predictions in complex Reservoirs: SPE Reservoir Evaluation & Engineering: v.5, no. 3, p.237-248.

Lonoy, A., 2006, Making sense of carbonate pore systems: American Association of Petroleum Geologists Bulletin, v. 90, no. 1, p. 1381-1405.

Mancini, E.A., and D.J. Benson, 1980, Regional stratigraphy of Upper Jurassic Smackover carbonates of southwest Alabama: Gulf Coast Association of Geological Societies Transactions, v. 30, p. 151-163.

Mancini, E.A., R.M. Mink, B.L. Bearden, and R.P. Wilkerson, 1985, Norphlet Formation (Upper Jurassic) of southwestern and offshore Alabama; environments of deposition and petroleum geology: American Association of Petroleum Geologists Bulletin, v. 69, p. 881-898.

Mancini, E.A., Tew, B.H., and Mink, R.M., 1990, Jurassic sequence stratigraphy in the Mississippi Interior Salt Basin of Alabama: Gulf Coast Association of Geological Societies Transactions, v. 40, p. 521-529.

Mancini, E. A., and Parcell, W. C., 2001, Outcrop analogs for reservoir characterization and modeling of Smackover microbial reefs in the northeastern Gulf of Mexico: Gulf Coast Association of Geological Societies Transaction, v. 51, p. 207–218.

Mancini, E.A., Parcell, W.C., Puckett, T.M., and Benson, D.J., 2003, Upper Jurassic (Oxfordian) Smackover carbonate petroleum system characterization and modeling, Mississippi interior salt basin area, northeastern Gulf of Mexico, USA: Carbonates and Evaporites, v.18, no.2, p. 125-150.

Mancini, E.A., Blasingame, T.A., Archer, R., Panetta, B.J., Haynes, C.D., and Benson, D.J., 2004, Improving hydrocarbon recovery from mature oil fields producing from carbonate facies through integrated geoscientific and engineering reservoir characterization and modeling studies, Upper Jurassic Smackover Formation, Womack Hill Field (Eastern Gulf Coast, USA): American Association of Petroleum Geologists Bulletin, v. 88, p. 1629-1651.

Mancini, E.A., Llinas, J.C., Parcell, W.C., Aurell, M., Badenas, B., Leinfelder, R.R., and Benson, D.J., 2004, Upper Jurassic thrombolite reservoir play, northeastern Gulf of Mexico: American Association of Petroleum Geologists Bulletin, v. 88, no. 11, p. 1573-1602.

Mancini, E.A., Parcell, W.C., and Ahr, W.M., 2006, Upper Jurassic Smackover thrombolite buildups and associated nearshore facies, southwest Alabama: Gulf Coast Association of Geological Transactions, v. 56, p. 551-563.

Mancini, E.A., Li, P., Goddard, D.A., Ramirez, V. and S.U. Talukdar, 2008, Mesozoic (Upper Jurassic-Lower Cretaceous) deep gas reservoir play, central and eastern

Gulf coastal plain: Associaton of Petroleum Geologists Bulletin, v. 92, p. 283-308.

Mancini, E.A., Parcell, W.C., Ahr, W.M., Ramirez, V.O., Llinas J.C., and Cameron, M., 2008, Upper Jurassic updip stratigraphic trap and associated Smackover microbial and nearshore carbonate facies, eastern Gulf coastal plain: American Associaton of Petroleum Geologists Bulletin, v. 88, p. 409-434.

Mann, S.D., 1988, Subaqueous evaporates of the Buckner Member, Haynesville Formation, northeastern Mobile County, Alabama: Gulf Coast Association of Geological Societies Transactions, v. 38, p. 187-196.

Mathisen, T., Lee, S. H., and Datta-Gupta, A., 2003, Improved Permeability Estimates in Carbonate Reservoirs Using Electrofacies Characterization: A Case Study of the North Robertson Unit, West Texas, SPE Reservoir Evaluation & Engineering, v. 6, no. 3, p. 176-184.

Ridgway, J. G., 2010, Upper Jurassic (Oxfordian) Smackover facies characterization at Little Cedar Creek field, Conecuh County, Alabama: MSc. Thesis, The University of Alabama, Tuscaloosa, Alabama, 128p..

Salvador, A., 1987, Late Triassic-Jurassic paleography and origin of Gulf of Mexico basin: American Association of Petroleum Geologists Bulletin, v. 71, p. 419-451.

Tolson, J.S., C.W. Copeland, and B.L. Bearden, 1983, Stratigraphic profiles of Jurassic strata in the western part of the Alabama Coastal Plain: Geological Survey of Alabama Bulletin 122, 425 p.

APPENDIX I

	Permit	Well Name	Operator	Well Status	Raster Logs	LAS Logs	Survey Data	Core Data	PERM Predicted	Sw Predicted	Core Shift
1	10560	CEDAR CREEK LAND & TIMBER CO. 30-1 #1	Pruet Production Co.	PA	Available	Not Available	Available	Available	No	No	Core not used
2	11963	CEDAR CREEK LAND & TIMBER 19-15	Pruet Production Co.	PR	Available	Not Available	Available	Available	No	No	Core not used
3	12872	CEDAR CREEK LAND AND TIMBER 20-12	Pruet Production Co.	CV	Available	Not Available	Not Available	Available	No	No	Core not used
4	13176	MCCREARY 20-6	Pruet Production Co.	PR	Available	Not Available	Available	Available	No	No	Core not used
5	13177	CEDAR CREEK LAND AND TIMBER 20-7	Pruet Production Co.	PR	Available	Not Available	Available	Available	No	No	Core not used
6	13301	CEDAR CREEK LAND & TIMBER 21-4	Midroc Operating Company	CV	Available	Not Available	Available	Available	No	No	Core not used
7	13438	CEDAR CREEK LAND & TIMBER 16-14	Pruet Production Co.	PR	Available	Available	Available	Available	Yes	Yes	-17
8	13439	MCCREARY 21-1	Pruet Production Co.	PR	Available	Available	Available	Available	Yes	Yes	-5
9	13472	PUGH 22-2	Pruet Production Co.	PR	Available	Available	Available	Available	Yes	Yes	1.85
10	13473	PUGH 17-9	Midroc Operating Company	CA	Not Available	Not Available	Not Available	Not Available	No	No	0
11	13510	CEDAR CREEK LAND & TIMBER 16-16	Pruet Production Co.	PR	Available	Available	Available	Available	Yes	Yes	0
12	13514	OVERBY 15-12	Midroc Operating Company	CA	Not Available	Not Available	Not Available	Not Available	No	No	0
13	13583	PUGH 22-3	Midroc Operating Company	CV	Available	Available	Available	Available	Yes	Yes	0
14	13588	JOHNSTON ESTATE 22-15	Midroc Operating Company	CA	Not Available	Not Available	Not Available	Not Available	No	No	0
15	13589	SANDERS 23-1	Pruet Production Co.	PR	Available	Available	Available	Available	Yes	Yes	29.5
16	13625	PRICE 14-12	Pruet Production Co.	PR	Available	Available	Available	Available	Yes	Yes	0
17	13670	TISDALE 14-16	Pruet Production Co.	PR	Available	Available	Available	Available	Yes	Yes	1
18	13697	FINDLEY 23-3	Pruet Production Co.	PR	Available	Available	Available	Available	No	No	0
19	13746	TISDALE 13-13	Pruet Production Co.	PR	Available	Available	Available	Available	Yes	Yes	-2.5
20	13770	OVERBY 15-14	Pruet Production Co.	PR	Available	Available	Available	Available	Yes	Yes	-11
21	13906	Horton 14-7	Pruet Production Co.	PR	Not Available	Available	Available	Available	Yes	Yes	3
22	13907	Oliver 20-15	Pruet Production Co.	PR	Available	Available	Available	Available	Yes	Yes	-6
23	13976	Craft-Mack 8-7 #1	Sklar Exploration Company, L.L.C.	DA	Available	Available	Available	Not Available	No	No	No Core data
24	14112	Tisdale 13-5	Pruet Production Co.	PR	Available	Available	Available	Available	Yes	Yes	0
25	14113	McCreary 13-16	Midroc Operating Company	CA	Not Available	Not Available	Not Available	Not Available	No		No Core data
26	14114	McCreary 13-1	Pruet Production Co.	PR	Available	Available	Available	Available	Yes	Yes	-0.5
27	14155	Whatley 14-6	Pruet Production Co.	PR	Available	Available	Available	Available	Yes	Yes	8.5
28	14181	McCreary 12-16	Pruet Production Co.	PR	Available	Available	Available	Not Available	No	No	No Core data
29	14216	Cedar Creek Land and Timber 15-10	Midroc Operating Company	DA	Not Available	Available	Available	Available	Yes	Yes	-5.5
30	14251	Cedar Creek Land and Timber 15-8	Pruet Production Co.	PR	Available	Available	Available	Available	Yes	Yes	0
31	14270	Cedar Creek Land and Timber 21-12	Pruet Production Co.	PR	Available	Available	Available	Available	Yes	Yes	4
32	14305	Horton 11-16	Pruet Production Co.	PR	Available	Available	Available	Not Available	No	No	No Core data
33	14309	McCreary 13-16	Pruet Production Co.	PR	Available	Available	Available	Available	Yes	Yes	0
34	14325	Craft-Mack 7-2 #1	Sklar Exploration Company, L.L.C.	PR	Available	Available	Available	Available	Yes	Yes	3.5
35	14358	Cedar Creek Land and Timber 21-10	Pruet Production Co.	PR	Available	Available	Available	Available	Yes	Yes	0
36	14360	McCreary 7-11	Pruet Production Co.	PR	Available	Available	Not Available	Available	Yes	Yes	0
37	14484	Craft-Cedar Creek Land & Timber, Inc. 5-5 #1	Sklar Exploration Company, L.L.C.	PR	Available	Available	Available	Available	No	No	3.2
38	14545	McCreary 18-6	Pruet Production Co.	PR	Available	Available	Available	Available	No	No	-7.8
39	14692	Cedar Creek Land and Timber 15-6	Pruet Production Co.	PR	Available	Available	Available	Available	Yes	Yes	8.2
40	14708	Horton 11-14	Midroc Operating Company	CV	Available	Available	Available	Available	No	No	9.2
41	14824	Pugh 22-12	Pruet Production Co.	TA	Available	Available	Available	Available	Yes	Yes	-2.4
42	14926	McCreary 7-9	Pruet Production Co.	PR	Available	Available	Available	Available	Yes	Yes	12
43	14965	McCreary 18-2	Pruet Production Co.	PR	Available	Available	Available	Available	Yes	Yes	-1
44	15000	McCreary 7-6	Pruet Production Co.	PR	Available	Available	Available	Available	Yes	Yes	1.6

#	ID	Well Name	Operator	Type							
45	15064	Horton 6-14	Pruet Production Co.	PA	Available	Available	Available	Available	Yes	Yes	-0.6
46	15165	Tisdale 23-9	Pruet Production Co.	PR	Available	Available	Available	Available	Yes	Yes	-15
47	15219	Cedar Creek Land and Timber 17-7	Midroc Operating Company	DA	Available	Available	Available	Available	Yes	Yes	-16.7
48	15357	Craft-Ralls 8-12 #1	Sklar Exploration Company, L.L.C.	PA	Available	Available	Available	Available	Yes	Yes	8
49	15413	Craft-Ralls 5-10 #1	Sklar Exploration Company, L.L.C.	PA	Available	Available	Available	Available	Yes	Yes	4.6
50	15415	Jackson 27-6	Pruet Production Co.	PR	Available	Available	Available	Available	No	No	Core not used
51	15416	Ralls 19-9	Midroc Operating Company	DA	Available	Available	Available	Available	Yes	Yes	-1.5
52	15418	Craft-Mack 8-2 #1	Sklar Exploration Company, L.L.C.	PR	Not Available	Available	Available	Available	No	No	10
53	15454	Mack 17-2	Pruet Production Co.	PR	Available	Available	Available	Available	Yes	Yes	3
54	15493	Craft-Ralls 5-8 #1	Sklar Exploration Company, L.L.C.	PR	Not Available	Available	Available	Available	Yes	Yes	9.5
55	15497	Craft-Ralls 4-5 #1	Sklar Exploration Company, L.L.C.	PR	Available	Available	Available	Available	Yes	Yes	12.7
56	15540	Cedar Creek Land & Timber 23-13 #1	Midroc Operating Company	DA	Available	Available	Available	Available	Yes	Yes	Core not used
57	15703	Cedar Creek Land & Timber 16-10	Pruet Production Co.	PR	Not Available	Available	Available	Available	Yes	Yes	13
58	15710	Lewis Estate 27-7	Pruet Production Co.	PR	Available	Available	Available	Available	Yes	Yes	63.6
59	15731	Craft-Mack 17-4 #1	Sklar Exploration Company, L.L.C.	PR	Available	Available	Available	Available	Yes	Yes	12.72
60	15771	McMillan 17-12	Pruet Production Co.	TA	Not Available	Available	Available	Available	Yes	Yes	1.8
61	15772	Cedar Creek Land & Timber 9-12	Pruet Production Co.	PR	Not Available	Available	Available	Available	Yes	Yes	-2
62	15852	Nick Ross 24-11 #2	Columbia Petroleum LLC	PR	Not Available	Not Available	Available	Not Available	No	No	No Core data
63	15869	Hamiter 17-16	Pruet Production Co.	PR	Not Available	Available	Available	Available	Yes	Yes	-2
64	15924	Kendall Lands 24-10	Pruet Production Co.	PR	Not Available	Available	Available	Available	Yes	Yes	2.5
65	15934	Johnston-Stewart 32-12 #1	Sklar Exploration Company, L.L.C.	DA	Not Available	Available	Available	Available	Yes	Yes	3.8
66	16053	Cedar Creek Land & Timber 23-3	Pruet Production Co.	PR	Available	Available	Available	Available	Yes	Yes	4
67	16073	Hamiter 16-13	Midroc Operating Company	DA	Not Available	Available	Available	Available	Yes	Yes	8.6
68	16091	Cedar Creek Land & Timber 14-14	Pruet Production Co.	PR	Not Available	Available	Available	Available	No	No	
69	16115	Craft-Ralls 33-7 #1	Sklar Exploration Company, L.L.C.	PR	Not Available	Available	Available	Available	Yes	Yes	-0.5
70	16135	Craft-Soterra LLC 27-6 #1	Sklar Exploration Company, L.L.C.	PR	Not Available	Available	Available	Available	Yes	Yes	-2
71	16174	Craft-Ralls 33-6 #1	Sklar Exploration Company, L.L.C.	PR	Available	Available	Vertical	Available	Yes	Yes	-3
72	16175	Cedar Creek Land & Timber 13-13	Midroc Operating Company	PA	Not Available	Not Available	Available	Available	No	No	Core not used
73	16237	Cedar Creek Land & Timber 14-15	Pruet Production Co.	PR	Not Available	Available	Available	Available	Yes	Yes	-1.4
74	16293	Craft-Smurfit-Stone 27-12 #1	Sklar Exploration Company, L.L.C.	PR	Available	Available	Available	Available	No	No	Core not used
75	16347	Barlow 30-3	Pruet Production Co.	AC	Not Available	Available	Available	Available	Yes	Yes	14.8
76	16570	Cedar Creek Land & Timber 21-10, 4-13	Pruet Production Co.	PR	Not Available	Not Available	Not Available	Not Available	No	No	No Core data
77	16583	Boothe & Casey 29-8	Pruet Production Co.	PR	Not Available	Not Available	Not Available	Not Available	No	No	No Core data
78	12872-GI-07-01	Cedar Creek Land And Timber 20-12 GI	Pruet Production Co.	AC	Not Available	Not Available	Not Available	Not Available	No	No	No Core data
79	13301-GI-07-02	Cedar Creek Land & Timber 21-4 GI	Pruet Production Co.	AC	Not Available	Not Available	Not Available	Not Available	No	No	No Core data
80	13583-GI-10-02	PUGH 22-3	Pruet Production Co.	AC	Available	Not Available	Not Available	Not Available	No	No	No Core data
81	13729-B	STUART 15-15	Pruet Production Co.	PR	Available	Available	Available	Available	Yes	Yes	-6.7
82	14069-B	Tisdale 24-3	Pruet Production Co.	PR	Available	Available	Available	Available	Yes	Yes	-9
83	14301-B	Horton 12-14	Pruet Production Co.	PR	Available	Available	Available	Available	Yes	Yes	3.8
84	14600-B	Craft-Evers 1-16 #1	Sklar Exploration Company, L.L.C.	DA	Available	Available	Available	Available	No	No	-9.7
85	14646-B	McCreary 12-8	Pruet Production Co.	PR	Available	Available	Available	Available	Yes	Yes	0
86	14652-B	McCreary 24-1	Pruet Production Co.	PR	Available	Available	Available	Available	Yes	Yes	0
87	14708-SWD-07-01	Horton 11-14 SWDW	Pruet Production Co.	AC	Not Available	Not Available	Not Available	Not Available	No	No	No Core data
88	14740-B	Harper 18-11	Midroc Operating Company	DA	Not Available	Available	Available	Available	Yes	Yes	-9.3

89	14740-B-1	Harper 18-12 #1	Pruet Production Co.	PR	Available	Available	Available	Available	Yes	Yes	-11
90	15068-B	Horton 6-15	Midroc Operating Company	PA	Available	Available	Available	Available	Yes	Yes	12.6
91	15068-B-1	Horton 6-16	Pruet Production Co.	AC	Not Available	Available	Available	Available	Yes	Yes	-5.2
92	15159-B	Craft-Brye 8-4 #1	Sklar Exploration Company, L.L.C.	PR	Available	Available	Available	Available	Yes	Yes	10
93	15166-B	Cedar Creek Land & Timber 19-2	Pruet Production Co.	PR	Available	Available	Available	Available	Yes	Yes	1
94	15263-B	Craft-Ralls 5-14 #1	Sklar Exploration Company, L.L.C.	PR	Available	Available	Available	Available	Yes	Yes	13.8
95	15496-B	Craft-Ralls 4-12 #1	Sklar Exploration Company, L.L.C.	PR	Available	Available	Available	Available	Yes	Yes	1.4
96	15540-B	Craft-Drakeford et al 33-13 #1	Sklar Exploration Company, L.L.C.	DA	Available	Available	Available	Not Available	Yes	Yes	No Core data
97	15540-B-1	Craft-Ralls 33-14 #2	Sklar Exploration Company, L.L.C.	PR	Available	Available	Available	Available	Yes	Yes	10.8
98	15591-B	Craft-Ralls 33-15 #1	Sklar Exploration Company, L.L.C.	TA	Available	Available	Available	Available	Yes	Yes	3
99	15604-B	Landreneau 18-10 #1	Pruet Production Co.	PR	Available	Available	Available	Available	No	No	14.8
100	15614-B	Craft-Ralls 4-2 #1	Sklar Exploration Company, L.L.C.	DA	Available	Available	Available	Available	Yes	Yes	12.6
101	15614-B-1	Craft-Ralls 4-2 #1-A	Sklar Exploration Company, L.L.C.	PR	Not Available	Available	Available	Available	Yes	Yes	-2.5
102	15747-B	Craft-Ralls 33-8 #1	Sklar Exploration Company, L.L.C.	DA	Available	Available	Available	Available	Yes	Yes	15.7
103	15794-B	Craft-Salter 8-15 #1	Sklar Exploration Company, L.L.C.	DA	Available	Not Available	Available	Available	Yes	Yes	3.6
104	15868-B	Cedar Creek Land & Timber 19-3	Midroc Operating Company	DA	Not Available	Available	Available	Available	Yes	Yes	-5.6
105	16011-B	Hamiter 20-3	Pruet Production Co.	PR	Not Available	Available	Available	Available	Yes	Yes	8
106	16073-B	Hamiter 16-12	Midroc Operating Company	DA	Not Available	Available	Available	Available	Yes	Yes	3.6
107	16166-B	Cedar Creek Land & Timber 22-8	Pruet Production Co.	PR	Not Available	Available	Available	Available	Yes	Yes	0
108	16175-B-1	Cedar Creek Land & Timber 13-12 ST	Pruet Production Co.	PR	Not Available	Available	Available	Not Available	No	No	No Core data
109	16202-B	Cedar Creek Land & Timber 22-16	Pruet Production Co.	PR	Not Available	Available	Available	Available	Yes	Yes	0
110	16223-B	Craft-Soterra LLC 27-2 #1	Sklar Exploration Company, L.L.C.	PR	Available	Not Available	Available	Available	No	No	Core not used
111	16238-B	Cedar Creek Land & Timber 23-12	Pruet Production Co.	PR	Not Available	Available	Available	Available	Yes	Yes	3.3
112	16254-B	Cedar Creek Land & Timber 23-2	Pruet Production Co.	PR	Not Available	Available	Available	Available	Yes	Yes	1
113	16327-B	Craft-Ralls 28-16 #1	Sklar Exploration Company, L.L.C.	PR	Not Available	Available	Available	Available	Yes	Yes	0

VITA

Name: Sharbel Salam Al Haddad

Email Address: sharbel.alhaddad@neo.tamu.edu

Education: B.S., Petroleum Studies, American University of

                              Beirut, 2004

                              M.S., Geology, American University of

                              Beirut, 2007

                              M.S., Geology (with emphasis in Petroleum Geology),

                              Texas A&M University, 2012

Experience: Paradigm, Dubai- UAE- Geomodeling consultant, 2007-2010

                              ExxonMobil, Houston, Texas- Summer intern, 2011

                              Currently with ExxonMobil- Houston, Texas